The effect of copper as a chemical promoter on the performance of a cobalt based Fischer-Tropsch Synthesis catalyst

Gert Stefanus van Wyk

Department of Chemical Engineering

University of Cape Town

Rondebosch

Cape Town

South Africa

The effect of copper as a chemical promoter on the performance of a cobalt based Fischer-Tropsch Synthesis catalyst

By

Gert Stefanus van Wyk - B. Eng. Chemical

Submitted to the University of Cape Town in partial fulfilment of the requirements for the degree of

Master of Engineering

Department of Chemical Engineering

University of Cape Town

Rondebosch

Cape Town

South Africa

28 April, 2000

ACKNOWLEDGEMENTS

I would like to thank Prof. Mark Dry and Dr. Eric van Steen for the support and encouragement that they have given me throughout the course of this work, for helping me focusing and achieving goals.

The Department of Chemical Engineering for giving me the opportunity for the ongoing education of myself and the research field.

I woukd like to thank Sasol for the postgraduate funding received, and trust that this work may serve as a suitable reward for their investment.

Thank you to my parents, Paul and Ria, for the personal support, help and opportunities that they have given me throughout my life. I truly appreciate it and I am very proud to be the son of such great parents.

SYNOPSIS

The most common Fischer-Tropsch catalysts are group VIII metals (Co, Ru and Fe). Iron catalysts are commonly used because of their low costs in comparison to other active metals. Alkali-promoted iron catalysts have been applied industrially for the Fischer-Tropsch synthesis for many years. Iron catalysts are often promoted with Cu, which increases the rate of reduction, enabling a lower reduction temperature [M. Dry, 1981]. In recent years more emphasis has been placed on catalyst productivity and selectivity as a criteria in choice of Fischer-Tropsch (FT) catalysts. Cobalt-based catalysts appear to provide the best compromise between performance and cost for the synthesis of hydrocarbons [Iglesia, 1997]. In the light of the fact that copper is used as a promoter for the iron catalyst and that the industry is looking at a commercial FT synthesis cobalt catalyst, it is essential to re-investigate the effect of copper on a cobalt catalyst

Copper has an effect on the overall activity of iron and cobalt [Kolbel, 1951, J. Schwank, 1991], but the reasons are not clearly understood. In the present study the role of copper as a promoter on the performance of 16.67% (wt) Co/SiO_2 is investigated with TPR, CO chemisorption, TEM and FT synthesis. The supported catalysts used in this study were prepared by impregnating a silica support with an aqueous solution of cobalt nitrate, using the incipient wetness technique. Drying and activation of the cobalt precursor followed impregnation. The stepwise impregnation of different amounts of copper {0%(wt) to 1.6%(wt)} were done on a master batch of the impregnated cobalt catalyst. This copper promoted catalysts was compared to the master batch of unpromoted catalyst.

The catalyst characterizations showed no apparent effect on the physical and chemical properties of the cobalt catalyst. The TPR-spectra showed a clear shift in the peaks to lower temperatures with an increase in copper content. This is due to a higher rate of reduction with an increase in copper content. It is proposed that H_2 adsorbs dissociatively on copper and thereby acts as a source of H_2 for the reduction of the cobalt oxide, and thereby increases the rate of reduction. In addition, the reduction of the copper oxide may form a 'hot spot' and

thereby increase the temperature of a certain region on the metal, and also increase the rate of reduction.

There was a significant influence on the FT performance of the catalyst. The activity of the cobalt catalyst decreased with an increase in copper loading. The addition of copper showed no significant effect on the metal surface area as well as on the dispersion. Copper has a higher tendency than cobalt to migrate to the surface, because of copper metal's higher mobility. It is speculated that because the copper is more mobile than cobalt the copper spreads itself over the cobalt surface. This would result in lowered amount of exposed cobalt surface atoms. Cobalt adsorbs CO dissociatively and is therefore active for FT synthesis, in contrast copper adsorbs CO associatively and is active for methanol formation [van der Laan, 1999]. This could explain why copper addition lowered the observed FT activity without lowering the measured CO chemisorption.

The products showed a typical Anderson-Schultz-Flory-distribution with the alpha values decreasing with an increase in copper content. The reason for the decrease in the alpha values with increasing copper content is not clear. It may be speculated that compared to cobalt, the relative adsorption strengths of CO and H_2 on copper are different. If H_2 adsorbs relatively more strongly on copper and if hydrogen spillover then occurs onto the cobalt surface, the latter would become more hydrogenating, resulting in lower olefin to paraffin ratios and an increase in the probability of chain termination, yielding the observed lower alpha values. The latter would explain the increase in methane selectivity and the decrease in the C_{5+} selectivity.

TABLE OF CONTENTS

LIST OF FIGURES

LIST OF TABLES

1. LITERATURE REVIEW

1.1 Introduction

The Fischer-Tropsch synthesis is a surface-catalyzed polymerisation process that uses CH_x monomers, formed by hydrogenation of adsorbed CO, in order to produce hydrocarbons with a broad range of chain length [E. Iglesia, 1997]. This process uses coal or natural gas as a source of CO to be converted into gasoline, diesel oil, wax, alcohols and alkenes.

1.2 The economic relevance of the process

Changes in the environmental demands, technological developments and fossil energy reserves have led to a growth in the actual interest in the Fischer-Tropsch synthesis (FTS). It is perhaps the most promising source of chemicals and fuels from non-petroleum based sources such as coal and natural gas. It is also important to note that currently natural gas is under-utilized and reserves are increasing. Due to energy saving policies and CO_2 emissions being blamed for global warming, flaring of associated natural gas has been charged with taxes. In areas where there are large natural gas and shrinking petroleum reserves and environmental demands, the gas can be converted into shippable hydrocarbon liquids by means of FTS [M.E. Dry, 1996].

At present chemicals and fuels are predominantly produced from crude oil. The price of petroleum crude has varied considerably over the last 30 years (see figure 1.1)

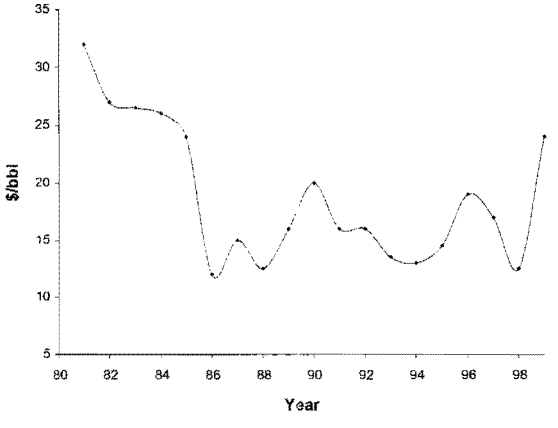

Figure 1.1: Petroleum crude oil prices

Presently, South Africa, is the only coal based FTS industrial developer. The reason for the viability of the Sasol plant is the fact that Sasol 2 and 3 came on line in the early 80's when the price of crude was high (see figure1.1) and fairly inexpensive coal was available for coal gasification. Syngas is made chiefly from natural gas or petroleum crude and presently syngas derived from natural gas is much cheaper than derived from coal.

Table 1.1: Coal and natural gas compared to oil.

Petroleum crude	Natural gas	Coal
- homogeneous liquid	- homogeneous fluid	- heterogeneous
- fairly narrow range i.t.o. composition: 82-87% carbon, 12-15% hydrogen, rest nitrogen, sulfur and oxygen	- purified natural gas composition: > 90% methane	- wide range of composition: 65-95% carbon, 2-6% hydrogen, 2-30% oxygen, 1-13% sulfur and up to 2% nitrogen
- H/C ratio is about 2	- no inorganic impurities	

1.2 Historical Background

Science, technology, business and politics mutually influenced the history of the Fischer-Tropsch process.

In 1902 Sabatier and Senderens discovered that carbon monoxide and hydrogen could form methane on nickel and cobalt catalysts [P. Sabatier et al.,1902]. After that, Orlov was the first to observe the formation of higher hydrocarbons [E.I Orlov, 1908]. In 1913 a BASF-patent reported that at high pressures and with cobalt catalysts, liquid products could be obtained in appreciable amounts [Patent BASF, 1913]. Fischer and Tropsch reported in 1923 that iron promoted by alkalis could produce liquid fuels from carbon monoxide and hydrogen, at high pressures [F. Fischer, H Tropsch, 1923]. Fundamental and technological research on F.T.S. flourished prior to and during the World War II, because of Germany having no oil fields. In the USA there was also a short period (1945-1955) of interest in the FTS, which resulted from a fear that the production of crude oil and the discovery of new oil fields would be unable to keep pace with the expected world-

wide growth in motor transport. After 1955, not much research was done on the FTS, but the disturbances in oil supply in 1973 led to a revival. During this period there was a considerable growth in this field, partly also because of better techniques available. Strategic and political considerations were the reasons for further development of the FTS in South Africa during its political isolation before 1993. When the oil supply shock was over and the mere existence of alternatives to the oil and naphta-based processes kept oil prices under pressure, the support for research on FTS and other syngas reactions vanished once again. However, large-scale FTS is still used in South Africa.

1.2.1 Plant Development

Table 1.2: The FT plant development over the last 100 years [M.E. Dry]

Year	Country	Production	Syngas	Catalyst	
1938	Germany, nine FT plants	$600*10^3$ (t/a)	Coal	Cobalt based, Fixed bed catalyst	Shut down in 1945; Uneconomic
1944	Japan, three FT plants	$110*10^3$			
1950	Texas, Brownsville	$360*10^3$	CH_4	Iron based, Fluidised bed catalyst	Operated only briefly; Uneconomic- increase in price of natural gas.
1955	South Africa, Sasol One	$700*10^3$	Coal	Iron based, Fixed and Fluidized bed catalyst	Economically viable; - Perception that crude oil reserves running out resulted in a increase in crude oil price - Large reserves of coal , mined at a low price - Produce high price FT waxes
1980	South Africa, Sasol Two	2 and 3 $4200*10^3$	Coal	Iron based, Fluidized bed catalyst	Economically viable; Rise in crude oil prices in 1970's
1982	South Africa, Sasol Three	2 and 3 $4200*10^3$	Coal	Iron based, Fluidized bed catalyst	Economically viable
1985	New Zealand, Mobil	$600*10^3$	CH_4	ZSM-5 catalyst (MTG process)	
1992	South Africa, Mossgas	$900*10^3$	Natural gas	Iron based, Fluidized bed catalyst	Limited reserves of gas
1993	Malaysia, Shell	$500*10^3$	CH_4	Cobalt based, Fixed bed catalyst	

1.2.2 Reactor Technology

It is important to note that the performance of the FTS depends strongly on reaction temperature.

An increase in temperature:

- favors methane formation
- favors deposition of carbon and thereby deactivation of the catalyst (particularly with iron)
- and reduces the average chain length of the product molecules

Also an increase in temperature increases the FT reaction rate. The process is strongly exothermic (about 145 kJ per mole of carbon incorporated into a growing chain) and heat removal is a major part of the reactor design. Keeping the catalyst bed isothermal is not easily attained. The more isothermal the catalyst bed, the higher the average temperature can be.

The first large-scale reactors were low temperature fixed bed reactors operated during World War 2 in Germany. These reactors consisted of a box, which was divided into sections by vertical metal sheets and horizontal cooling tubes crossing the sheets, the catalyst being loaded between sheets and tubes. In 1955 Sasol One commissioned the first commercial ARGE reactors jointly developed by Ruhrchemie and Lurgi. Temperature control was achieved by the vaporization of water, which surrounded the catalyst containing tubes. The FT reactors used by Shell in Malaysia are also multitubular.

The use of slurry reactors for FTS was studied by Fischer and co-workers on a small scale but large-scale tests were first carried out by Kölbel when a unit was commissioned in 1953. Sasol also investigated the slurry reactor and in 1993, a simple yet efficient device for separating the suspended catalyst from the net wax production was successfully tested in a demonstration reactor. A commercial unit was subsequently built and commissioned.

The high temperature circulating fluidized bed reactors (CFB) developed by Kellog was used by Sasol for its first plant. The Sasol 2 and 3 CFB reactors as well as those used at

the Mossgas plant are improved versions of the Sasol 1 reactors. The fixed fluidized bed reactors were simpler to operate and were used in the FT plant, which operated briefly in Texas, with unknown reliability. Sasol started in 1996 with the process of replacing the CFB with the FFB units.

Table 1.3: Advantages and disadvantages of Multi-tubular fixed bed (MTFB) reactors compared to fluidized bed reactors.

Advantages	Disadvantages
- simple to operate.	- expensive to construct.
- can be used irrespective of whether the products are gaseous or liquids, or both.	- high gas compression costs.
- easy separation of liquid products from catalyst	- catalyst particle size cannot be too small
- less by H_2S poisoning due to the bulk of the H_2S being absorbed by the top layers of the catalyst, thus, the remainder of the bed remains unaffected.	- labour intensive to replace catalyst, - long downtime.

Table 1.4: Advantages and disadvantages of Two phase fluidized bed (FB) reactors compared to Multi-tubular fixed bed reactors.

Advantages	Disadvantages
- higher efficiency in heat exchange than MTFB.	- more complex to operate, particularly the circulating fluidized types, than MTFB
- low cost reactor and construction.	- effective separation of catalyst fines from the exhaust gas is not simple.
- low gas compression costs.	- more affected by H_2S poisoning than MTFB.
- can use small particle size. (<100 μ m)	
- easy removal and addition of catalyst, - short downtime. - near isothermal reaction zone	

Table 1.5: Advantages and disadvantages of Three phase slurry bed reactors compared to Multi-tubular fixed bed reactors.

Advantages	Disadvantages
- construction cost 40 % less.	- affected by H_2S poisoning
- low gas compression costs.	- limit to amount of catalyst loaded.
- can use small particle size. (< 100 μm)	
- easy removal and addition of catalyst,	
- short downtime.	
- near isothermal reaction zone.	

1.3 Catalysts for the FTS

Fischer-Tropsch synthesis needs a catalyst, which can adsorb CO and H_2, like the transition metals in group VIII. Vannice tested these catalysts and the results showed that Ru was the most active.

Metals in order of increasing specific activity:

$$Ru > Fe > Co > Rh > Ni > Ir > Pt > Pd$$

Vannice also tested the average molecular weight of the organic products.

Arranged according to descending chain length:

$$Ru > Fe > Ni > Co > Rh > Pd > Pt > Ir$$

This group of metals was tested at atmospheric pressure and not at optimum conditions for each catalyst, e.g. cobalt was tested at 240 ^{0}C with a H_2/CO ratio of 3 [Vannice, 1975]. The choice of relatively cheap Fe catalyst for pioneering German work is confirmed by these results (see table 1.6). Co-based catalysts were later preferred simply because they required considerably milder operating pressures than the Fe catalysts. The main differences between cobalt and iron as a catalyst is that the methane selectivity is generally higher for cobalt and readsorption of reactive product compounds is stronger for cobalt. With iron branching takes place as a primary branching reaction, while with cobalt, branching is mainly due to a secondary branching reaction [van Steen, 1993].

Table 1.6: Relative prices of metals (March 1989) [Rao V.U.S.,1992]

Metal	Price ratio
Fe	1
Co	230
Ni	250
Ru	31000
Rh	570000

Pichler identified common properties for the catalysts, which were active for FTS:

- They are active for hydrogenation reactions.
- They are capable of metal carbonyl formation.
- The FT reaction conditions (temperature, pressure) are not far from those where thermodynamics would allow the metals to be converted into metal carbonyls.

[Pichler et al., 1970]

Under synthesis conditions Fe readily forms oxides and several carbides. It has a stronger tendency than Co or Ni to produce elemental carbon. The formation of Co and Ni carbide is thermodynamically unfavored at FTS conditions (433-573 K). Ni is essentially a methanation catalyst while Co yields mainly straight-chain hydrocarbons. The water-gas shift activity is very low over Ni and Co. Ru produces high molecular weight species at low temperatures and carbides of Ru are unknown at typical FTS conditions. Although Mo is not a Group VIII metal, it exhibits moderate FT activity and its nitride and carbide show excellent alkene selectivity. Other group VIII metals, namely Rh, Re, Os, Pd, Pt and Ir yield mostly oxygenated compounds.

1.3.1 Cobalt as Fischer-Tropsch catalyst

The Fischer-Tropsch synthesis temperature for cobalt ranges from 190^0C to 210^0C. Olefins, particularly α -olefins, seem to be a primary product of FTS [Anderson, 1984]. Cobalt metal is more hydrogenating than alkalized iron and subsequently produces more methane and less olefins [M.E. Dry, 1996]. The water-gas-shift reaction activity for cobalt

catalyst is very low. Although cobalt is a more active catalyst for FTS, it is much more expensive than iron (see table 1.6).

1.3.2 Promoters

A promoter is a substance added to a catalyst to improve its activity and/or selectivity for a given reaction and/or to prolong the life of a catalyst. Promoters can be divided into structural and chemical promoters.

1.3.2.1 Structural promotion

Structural promoters facilitate the formation of a structure of high surface area during the preparation or pretreatment of the catalyst by dispersing the metal, inhibits sintering and inhibits the formation of metal-support interactions. Structural promoters stabilize the structure of the catalyst.

Rhenium is a structural promoter of supported Co catalysts. It acts by preventing agglomeration of CoO_x particles during calcination treatments, which leads to higher Co metal dispersions [E. Iglesia, 1997]

1.3.2.2 Chemical promotion

Chemical promoters enhance the activity of the catalyst by chemical interaction with the metal and thereby change the chemical nature of the surface.

Iron based catalysts require promotion by alkalis, K_2O is commonly used. Alkalis, as well as supports such as SiO_2 and Al_2O_3 determine the basicity of the catalyst. The effect of alkali promotion of cobalt is much less marked than for iron. Promoters influence the bond strength of hydrogen to metal. Addition of alkali metals to iron catalysts promotes electron transfer to the iron and inhibits hydrogen adsorption, because adsorption of hydrogen induces electron donation to the iron surface [Vannice, 1977, Dry, 1981]. The alkali addition increases the strength of CO chemisorption and so enhances its decomposition to C and O atoms. In agreement with this alkali promotion is known to

increase the rate of carbon deposition. The higher the surface concentration of C atoms, the higher the coverage by the CH_2 building blocks and thus the higher the probability of chain growth according to the proposed mechanisms [M.E. Dry, 1996]. For this reason there is an increase in selectivity of alkenes and long-chain hydrocarbons.

The F.T.S is also influenced by the addition of metal oxides to supported metals. For instance, vanadium, niobium, molybdenum, tungsten, chromium, lanthanum, thorium or cerium oxides cause an increase of the total activity and shifts in the selectivity when they are promoting Ru, Rh, Co, or Ni catalysts. The promoting effect of these oxides have been attributed to two phenomena: (i) the presence of partially reduced promoter oxides which provide binding sites for the oxygen end of the carbon monoxide molecule facilitating its decomposition and (ii) the coverage of the surface of the active phase by the promoter resulting in a decreased chemisorption capacity and in a restricted mobility of the adsorbed species [A.Guerrero-Ruiz et al., 1994].

The aim of bimetallic catalysts is to take advantage of possible synergetic effects between the two metals, and thus produce a higher active, selective and stable catalyst [Adesina, 1996]. The addition of another metal to cobalt increases the number of exposed Co sites. The second metal, in close approximity with Co, modifies either the strength of CoO_x-support interactions or the reducibility of CoO_x precursors. For example, the addition of Ru to Co/Al_2O_3, Co/SiO_2 and Co/TiO_2 catalyst decreases the temperature at which CoO_x precursors reduce to Co metal [E. Iglesia, 1993]. The addition of another metal can also increase the Fischer-Tropsch synthesis rate per exposed Co metal atom. Small amounts of Ru (Ru/Co = 0.007 atom ratio) increases FTS turnover rates on Co/SiO_2 and Co/TiO_2 catalysts [C. Mirodatos et al., 1995].

1.3.2.3 Copper as promoter

Copper has been widely used as one of the promoters for FTS on iron catalysts, particularly in slurry reactors [Kolbel and Ralek, 1980]. Its function is to decrease the temperature required for reduction of iron oxides [H.H. Storch et al., 1951;R.B. Anderson,

1956; R.B. Anderson et al., 1952]. If copper was not added to a precipitated iron catalyst, and the catalyst is reduced at higher temperatures to attain the same degree of reduction as when copper is present; the activity of the catalyst is inferior [M. Dry, 1981].

Only a few investigations have been reported for copper promotion of precipitated iron catalysts that contain no potassium. Kolbel observed an increase in the overall activity at very low levels (ca. 0.1 wt %) of copper promotion with no further effects at higher copper loading [Kolbel et al., 1951]. Wachs reported that product distributions do not change appreciably when copper is incorporated into an iron catalyst for experiments in a differential fixed bed reactor [Wachs et al., 1984]. The reasons for the increased catalyst activity on the iron catalyst with the addition of copper are not clearly understood. In 1951 H. Storch stated that the addition of copper to a cobalt catalyst is deleterious for the FTS reaction [H. Storch 1951]. Schwank stated in 1991 that a pronounced suppression of activity is observed when copper is added to iron or cobalt [J. Schwank, 1991]. Unfortunately no numbers were given for the effect of copper on the activity of the catalyst.

The effect of alloying Fisher-Tropsch catalyst with copper is dependent on the temperature range of the reaction. (see figure 1.2)

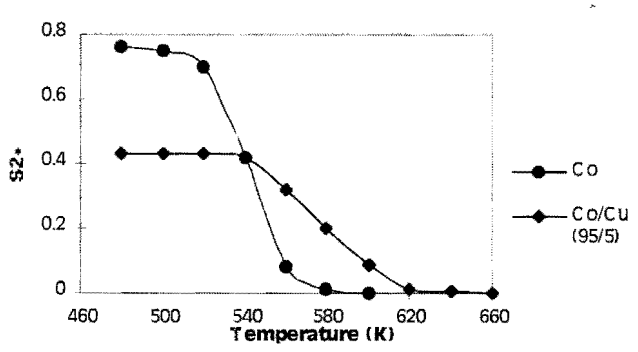

Fig 1.2: Selectivity S2+ as a function of temperature: pure Co and a 5% cobalt-copper alloy.

A conventional flow apparatus, working at about 1 atm. pressure was used to test the effect of adding copper to a unsupported Co metal catalyst. Selectivity of higher hydrocarbon production (S_{2+}) was defined as $S_{2+} = (2C_{2+} + 3C_{3+} + ...)/(C_1 + 2C_{2+} + 3C_{3+} + ...)$ where C_i is a molar concentration obtained from GLC peak heights after necessary recalculations. The same behavior as represented by figure 1.2 has also been found with Ni- and Ni-Cu-supported catayst. When catalysts prepared under identical or similar conditions are compared, results with supported catalysts fully confirm the picture obtained with unsupported catalysts.

1.3.3 Choice of support

The choice of support for FT catalysts is dictated by several considerations:

- inertness
- high surface area
- stability under reaction conditions
- porosity
- pH
- strong-metal support interaction; and
- low cost

The commonly used supports for FT catalysts are silica, alumina, titania, magnesia, zirconia and activated carbon. Zeolites have also been investigated as supports for FT catalysts [Anderson, 1975]

1.4 Fischer-Tropsch Product Spectrum

Linear hydrocarbons and some branched hydrocarbons are the major products formed in FTS. The linear hydrocarbon fraction contains mainly paraffins and olefins. Oxygenates are formed as a side product i.e. alcohols, aldehydes and ketones. In high temperature FTS some minor quantities of naphthenes and aromatics are formed.

For straight chain alkanes the generic equation is:

$$(2n+1)\ H_2 + n\ CO \rightarrow C_nH_{(2n+2)} + nH_2O$$

For straight chain alkenes the generic equation is:

$$2n\ H_2 + n\ CO \rightarrow C_nH_{2n} + n\ H_2O$$

and the reaction leading to alcohols is:

$$2n\ H_2 + n\ CO \rightarrow C_nH_{(2n+1)}OH + (n-1)\ H_2O$$

One of the principal objectives in FT technology is to control the selectivity of these products and this depends on the reaction conditions and catalyst composition.

1.5 Mechanisms

To understand the way in which syngas is converted to hydrocarbons one must take a closer look at the events occurring at the surface of the catalyst.

The products can be divided into primary products and secondary products. All the products formed by desorption without subsequent re-adsorption are primary products. Secondary reactions can alter the FTS selectivity by subsequent reactions of this primary products. [Iglesia *et al.*, 1993] (see figure 1.3)

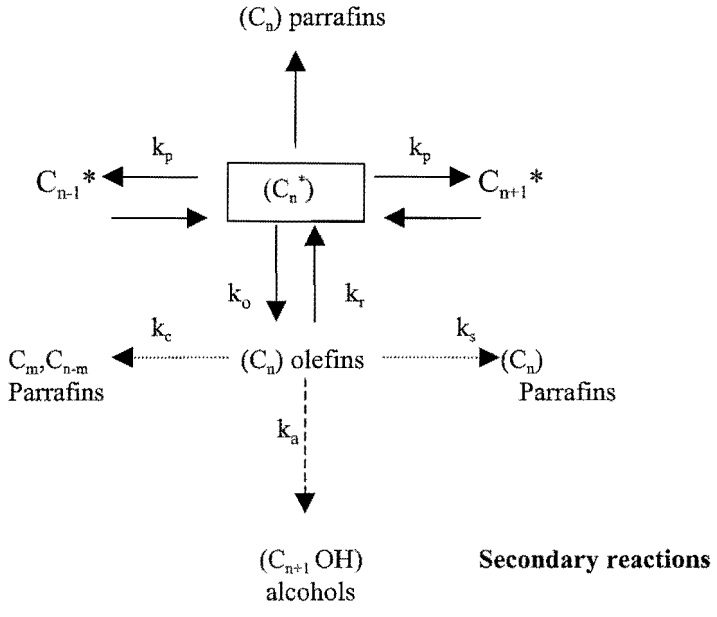

Figure 1.3: The chain growth and termination and secondary reactions in FTS on the cobalt catalyst. [Iglesia et al., 1993]

Cn*: adsorbed surface species with n carbon atoms,

kp: rate constant for chain termination,

ko: rate constant for olefin formation,

kr: rate constant for readsorption and

kc: rate of the cracking reaction

ka: rate of the hydroformulation reaction

ks: rate of the hydrogenation reaction

FTS has long been recognized as a polymerization reaction. Regarding FT chain growth, it can be visualized as a sequence of repeated reactions in which the C-O bond is split and hydrogen is added to carbon and to oxygen, and a new C-C bond is formed.

For one CH2 - group produced

$CO + 2H_2 \rightarrow (CH_2) + H_2O$

these 7 reactions are proposed

- associative adsorption of CO

- splitting of the C-O bond
- dissociative adsorption of $2H_2$
- transfer of 2H to the oxygen to yield H_2O
- desorption of H_2O
- transfer of 2H to the carbon to yield CH_2
- formation of a new C-C bond

The order of these steps are not fully understood; is the hydrogen added to the adsorbed CO first and thereby forming oxygen containing intermediates, or does the C-O bond split first, yielding hydrocarbon intermediates?

The three main mechanistic proposals are:

- surface carbide mechanism
- enol condensation mechanism
- CO-insertion mechanism

Fischer and Tropsch proposed the surface carbide mechanism in 1926. The assumption, on which their theory rests, is that CO adsorps dissociatively on the catalyst surface, to form surface carbide. The surface carbide is then partially hydrogenated forming carbene species.

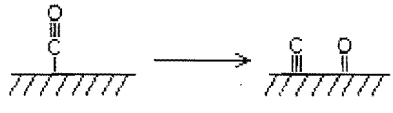

Figure 1.4: The dissociative adsorption of CO

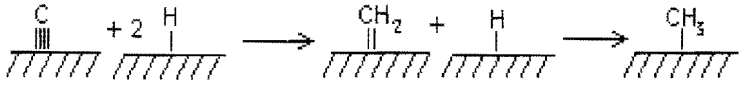

Figure 1.5: The hydrogenation of the surface carbide

The methylene group can undergo further reaction with hydrogen to form a methyl group on the catalyst surface. This methyl group then has the option of either desorbing by hydrogen addition or starting a new chain.

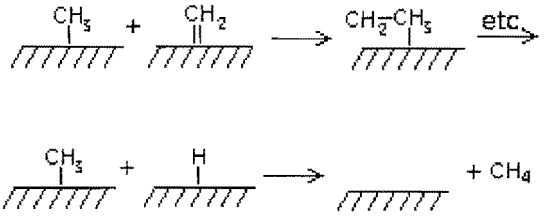

Figure 1.6: The methylene group undergoing chain growth and chain termination

In the enol condensation mechanism, proposed by Anderson, Emmet and their co-workers, C-C bonds are formed through a condensation reaction. Two hydroxymethylene surface species react by forming water and surface oxy species [Anderson, 1975]

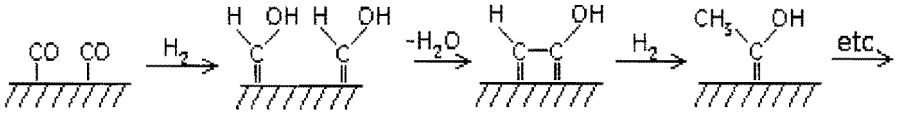

Figure 1.7: The self condensation of surface hydroxycarbene intermediates

The CO insertion mechanism is the third mechanism proposed by Pichler and Schulz (1970). In this mechanism propagation takes place via insertion of a CO into a metal-alkyl bond [Pichler and Schulz, 1970].

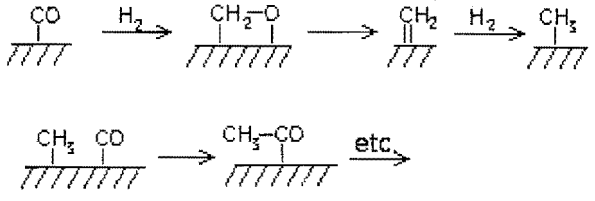

Figure 1.8: Chain growth by the insertion of CO

From the proposed mechanisms it is clear that the Fischer-Tropsch process can be described as a non-trivial surface-polymerisation reaction. The unique character of the system is well summarized by the surface-polymerization reaction in which one step of chain growth (on CH_2 unit) is performed through a set of reactions of hydrogen transfer, elimination of oxygen and formation of a new C/C bond.

According to Anderson, the distribution of n-paraffins can be described by the Anderson-Schultz-Flory (ASF) equation:

$m_n = (1-\alpha)\alpha^{n-1}$

where the growth probability factor α is independent of n and m_s is the mole fraction of a hydrocarbon with chain length n. α is defined by:

$$\alpha = \frac{R_p}{R_p + R_t}$$

where R_p and R_t are the rates of propagation and termination, respectively. α determines the total caron-number distribution of the FT products and the range of α is dependant on the reaction conditions and catalyst type. The ASF equation does not distinguish between different product types of the polymerization process. A semilogarithmic plot of the mole fraction against carbon number yields the well-known ASF-diagram, where the slope of the straigh line yields the chain growth probability α [Iglesia et al., 1993].

1.6 Effect of reaction parameters

The choice of reaction parameters is important for the optimization of any catalytic process. The type of reactor used in the process determines the range of applicable conditions due to physical constraints associated with the type of reactor.

1.6.1 Effect of temperature

The influence of temperature on the selectivity is consistent for all FT catalysts. With a higher temperature the chain growth probability decreases. This leads to an increase in the methane selectivity and a decrease in the hydrocarbon chain length. For example, nickel and ruthenium catalysts operating at low temperatures (< 190 ^{0}C) produce a high proportion of wax, but at higher temperatures (> 300 ^{0}C) methane is the main product formed. A Sasol fluidized iron catalyst showed all the trends mentioned above, namely, as the temperature increased the CH_4 selectivity increased and it also showed that the olefinity of the products and the alcohols and acids selectivities decreased. These results

also corresponded to product selectivities resulting from a temperature increase over a cobalt catalyst [M.E. Dry, 1981].

1.6.2 Effect of pressure

A increase in total pressure increases the chain growth probability, for example, increasing the operating pressure of a cobalt catalyst, from 0.1 MPa, to about 1.5 MPa shifted the hydrocarbon selectivity towards the heavier products [F. Martin, 1939]. Roelen found that over precipitated iron catyalysts, that up to about 2.0 MPa the wax selectivity increased with increased pressure and that there was little change in the olefinity of the liquid products [R.B. Anderson, 1956] The yield of oxygenate molecules increased with pressure. Friedman and Schlesinger investigated the influence of pressure up to 10.3 MPa over nitrided fused iron catalyst and showed all the trends mentioned above as well as a increase in oxygenate content [S. Friedman M.D. Schlesinger, 1964]. Changes in product spectrums with increased pressure can be attributed to increased partial pressures of reactants and products. Claeys et al [1997] showed that increased partial pressures of water over a slurry phase cobalt catalyst lead to significant changes in product composition, including suppressed methane formation, enhanced chain growth, and the inhibition of secondary olefin formation.

1.6.3 Effect of H_2/CO ratio

Evaluating the effect of the H_2/CO ratio indicates that a decrease in the H_2/CO ratio results in a higher average molecular weight hydrocarbon product and higher olefinicity. Anderson [1956] showed similar findings for a Co/Ni/ThO_2/Mn/Kieselguhr catalyst. A lower H_2/CO ratio resulted in lower methane selectivity and a higher olefin content. These results are understandable in that a catalyst surface preferentially covered with hydrogen favors chain termination. Thus the desired product selectivity is largely determined by the fractional surface coverage of CO, H_2, CO_2 and H_2O.

1.7 Objective of current research

In 1951 H. Storch stated that the addition of copper to a cobalt catalyst is deleterious for the FTS reaction [H. Storch 1951]. Schwank observed a pronounced suppression of activity when cobalt is added to iron or cobalt and Dry stated that the presence of copper in a cobalt catalyst increases the rate of decline of the catalyst's activity in FT synthesis [Schwank J., 1991, M. Dry, 1981].In the light of the fact that copper is used as a promoter for the iron catalyst and that the industry is looking at a commercial FTS Co catalyst, it is essential to re-investigate the effect of copper on a Co catalyst. Cu is mainly used to facilitate the reduction process with the iron catalyst. With Cu the reduction temperature can be lowered thereby decreasing the effect of sintering. Bukur observed no effect of copper on the product distribution and stated that additional studies with Fe/Cu catalyst are required in order to elucidate the role of copper in the FTS [H. Bukur, 1990].

The objective of the present study is to investigate the effect of copper on the FT Co catalyst. Can it be used as a reduction promoter and how will it effect the FTS activity and product spectrum?

2. EXPERIMENTAL

2.1 Catalyst Synthesis

A cobalt based catalyst appears to provide the best compromise between performance and cost for the synthesis of hydrocarbons [Iglesia, 1997]. The catalysts were prepared by means of incipient wetness due to the simplicity of the procedure and it is the most commonly employed method. Cobalt nitrate and copper nitrate were used as a precursor because it is simple to prepare and easy to decompose to cobalt and copper oxide respectively. The precursor was brought into contact with the support by means of impregnation. Silica was chosen because a lot is known about silica as a support and less carbonaceous deposit and interaction between metal and support occurs on Co/SiO_2 than on the Co/Al_2O_3 catalyst [Boskovic and Smith, 1997]. After depositing the metal precursor on the support the precursor was transformed into the required active component via calcination and reduction.

2.1.1 Determination of the support void volume

This was done to determine the amount of liquid that needs to be added to the support during the impregnation. The void volume that includes pore volume and interparticle void volume of the particles was determined by titrating accurately weighed masses of the silica support with deionised water, until a thin layer of water could be seen at the surface of the silica. The measured void volumes for selected supports are in very close agreement with calculated values of van Steen et al. (1996). Aldrich Chemical Company supplied the silica support (99 % purity). The physical characteristics of the support are listed in Table 2.1.

2.1.2 Preparation of supported catalyst

The metal salt $Co(NO_3)_2\ 6H_2O$ was dissolved in an appropriate volume of deionised water and then added to the silica support, to obtain a loading of 20g Co/100g SiO_2. The same procedure was followed for the preparation of 20g Cu/100g SiO_2 with $Cu(NO_3)_2\ 3H_2O$ as the metal salt. For the "co-impregnated" catalyst an appropriate amount of both metal

salts; $Co(NO_3)_2$ $6H_2O$ and $Cu(NO_3)_2$ $3H_2O$ were dissolved in an appropriate volume of deionised water and then added to the silica support, to obtain a loading of 20g Co/100g SiO_2. The cobalt nitrate and copper nitrate used had a purity greater than 99% and was supplied by Merck.

			Void volume	
	Surface area	Mean pore diameter	Calculated	Measured
	(m^2/g)	(Å)	(cm^3/g)	(cm^3/g
Davisil grade 646	300	150	2.25	2.3

Table 2.1: Characteristics of the Silica gel used

The impregnated samples were aged for 3 days at room temperature in a desiccator and subsequently dried in an oven at 90^{0}C for 1 hour. Drying resulted in the elimination of the water from the pores of the support [Perego and Villa, 1997].

2.1.3 Preparation of supported catalyst with promoter

The copper was added to the catalyst by means of a stepwise impregnation. The metal salt $Co(NO_3)_2$ $6H_2O$ was dissolved in an appropriate volume of deionised water and then added to the silica support, to obtain a loading of 20g Co/100g SiO_2. The impregnated samples were aged for 3 days at room temperature in a desiccator and then subsequently dried in an oven at 90^{0}C for 1 hour. The precursors were calcined in a fixed bed reactor at 380 ^{0}C for 6 hours in N_2 (60 ml (STP)/min). The heating rate was 10 ^{0}C/min. The correct amount of $Cu(NO_3)_2$ $3H_2O$ was then dissolved in an appropriate volume of deionised water and then added to the calcined catalyst, to obtain four different loadings of copper:
0.1g Cu/20g Co/100g SiO_2 ; 0.5g Cu/20g Co/100g SiO_2 ; 1g Cu/20g Co/100g SiO_2 and 2g Cu/20g Co/100g SiO_2. The copper nitrate used had a purity greater than 99% and was supplied by Merck. The catalyst precursor was aged for 3 days at room temperature in a desiccator and then subsequently dried in an oven at 90^{0}C for 1 hour.

2.2 Catalyst activation and treatment

The overall activity is related to the activation treatments that the cobalt catalysts undergo. The time and temperature of the drying, calcination and reduction influence the surface properties and extent of reduction of the cobalt catalyst. The active phase of the cobalt catalyst for the FTS is the metal phase. Calcination was followed by reduction of the catalyst.

2.2.1 Calcination

Calcination usually takes place in an oxidising environment, at temperatures higher than those used in the catalytic reaction. The cobalt nitrate precursor is calcined in N_2, the nitrate decomposes to HNO_3 and NO_x gases that serves as the oxidising atmosphere. During calcination several processes occur: loss of chemically bonded water or NO_2, decomposition of the precursor, modification of the surface (size of the oxide crystals increase) and the modification of the structure.

The precursors were calcined in a fixed bed reactor at 380 ^{0}C for 6 hours in N_2 (60 ml (STP)/min). The heating rate was 10 ^{0}C/min.

2.2.2 Reduction

All the catalysts were first dried by heating the catalysts to 100 ^{0}C in argon and then heated up at 2 ^{0}C/min., and reduced for 16 hours at 360 ^{0}C in pure hydrogen (60 ml (STP)/min).

2.3 Catalyst characterisation

Catalyst characterisation is a very important step in the design of a catalyst. It aids linking structural and electronic properties of the active compound with catalytic performance, which includes selectivity, activity and lifetime of the catalyst. The catalysts were characterised using thermochemical, adsorptive and spectroscopic techniques.

2.3.1 Temperature programmed reduction

This thermoanalytical technique measures the response of a solid as the temperature is changed in a reducing atmosphere. A linear rate of temperature increase is applied while passing a reducing gas over the catalyst bed. The objective of temperature programmed reduction (TPR) is to understand the behavior of the catalyst under reduction. TPR is particularly useful for the characterisation of metal oxide catalysts. The catalyst precursor is exposed to a flow of a reducing gas mixture, typically 5% hydrogen with nitrogen as the make up gas and the concentration of the reducing gas in the effluent gas stream is then monitored as a function of sample temperature. The metal oxides are reduced according to the following general reaction pathway:

$$MO + H_2 \rightarrow M + H_2O \qquad (1)$$

The thermodynamics of the reaction (1) as measured by the change in Gibbs free energy is:

$\Delta G = \Delta G^{\circ} + RT\ln (P_{H2O} / P_{H2})$

The high H_2/N_2 gas flow rates over the catalyst keeps the partial pressure of water low. Under these conditions, the reduction of the metal oxide remains thermodynamically favorable.

2.3.1.1 Temperature programmed reduction procedure

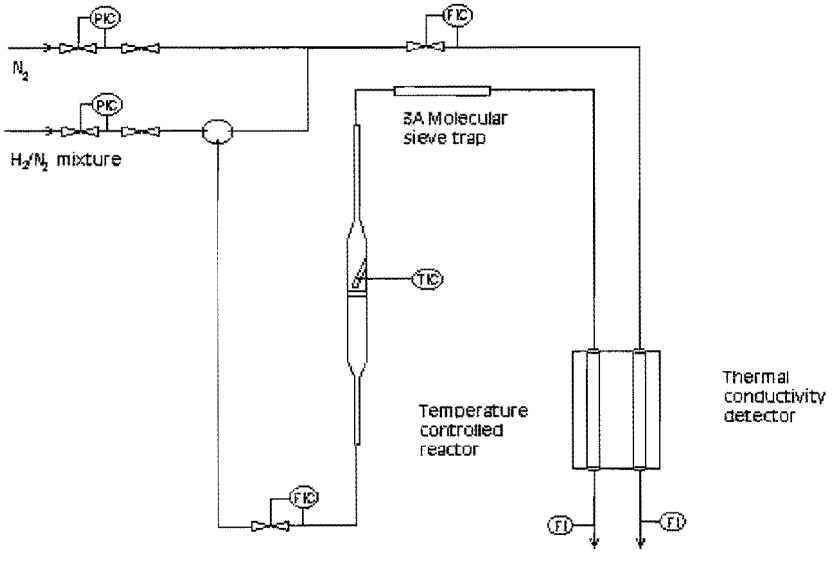

Figure 2.1: The flowsheet of the temperature programmed reduction apparatus

Approximately 0.15 g of catalyst was loaded on a porous fritt in a quartz mini reactor. The quartz reactor has a thermowell in which a thermocouple was inserted to control the temperature. A reducing gas consisting of 6% H_2 in N_2 was passed over the catalyst bed at 60 ml (STP)/min. The H_2/N_2 mixture was calibrated by temperature programmed reduction of pure copper oxide. The thermal conductivity of the reactor exit stream was measured with a thermal conductivity detector (TCD). The hydrogen consumption could be calculated from the change in thermal conductivity.

The catalyst was loaded in the reactor and then heated up in 60 ml (STP)/min. nitrogen, to 180 ^{0}C at 10^{0}C/min., and left for 1 hour. After cooling down the reactor to 100^{0}C at 5^{0}C/min., the TCD was left for 5 hours to stabilize. Upon obtaining a stable signal from the TCD, the gas stream was switched to 60 ml (STP)/min. H_2/N_2 and the temperature was raised linearly from 100 ^{0}C to 1000^{0}C at 10 ^{0}C/min. After reaching 1000 ^{0}C the temperature was kept for 10 minutes to ensure complete reduction.

2.3.2 Adsorptive characterisation techniques

The determination of surface area is considered to be an important requirement in catalyst characterisation, although the catalytic activity may not be directly related to the total surface area.

2.3.2.1 Carbon monoxide chemisorption

The measurement of the metal surface area of a supported metallic catalyst requires adsorption exclusively or predominately on the metal surface. In chemisorption measurements, the crux of the problem is how to determine the monolayer uptake from the experimental isotherm. Monolayer coverage under these conditions is assumed for the purpose of comparing the surface area of different catalysts. CO chemisorption does have the difficulty that the chemisorption stochiometry is variable because the proportion of chemisorbed species in the linear and bridged forms can vary, the former offering a chemisorption stoichiometry of one, the latter of two.

Measurements were performed using a Micrometrics ASAP 2000C apparatus. The catalyst precursor was heated at 10 ^{0}C/min up to 360 ^{0}C under hydrogen, and kept at this temperature for 16 hours. After reduction the catalyst was degassed for 2 hours at 10^{-5} torr in order to eliminate chemisorbed hydrogen. The temperature was then lowered to 30 ^{0}C while maintaining the vacuum. The amount of CO adsorbed was determined using the dual isotherm technique. Chemisorption isotherms were measured between 50 - 400 mm Hg. After completing the first isotherm the weakly adsorbed CO was eliminated by evacuating the sample for 30 minutes at 10^{-5} torr and then the second isotherm was obtained. The difference between the two isotherms gave the amount of CO irreversibly chemisorbed on the sample.

2.3.2.2 BET surface area measurements and pore radius distribution

The characterisation of a catalyst ideally includes the measurement of the total surface area of the support together with the measurement of the average pore diameter. The average pore diameter and the surface area of the support are related, and can be obtained from physical adsorption measurements. Surface area and mean pore diameter measurements were made by the BET method using nitrogen as an adsorbate.

2.3.3 Spectroscopic characterisation techniques

2.3.3.1 Transmission electron microscopy

Transmission electron microscopy allow the direct observation of catalyst morphology with magnification in the range of 10^{-4} - 10^{-10} m.

The catalyst samples were crushed and wetted with a few drops of distilled water. Copper grids with a thin film of carbon acting as a support for the specimen were floated on the droplets of the sample. Excess sample was blotted with filter paper and the sample was allowed to dry.

The samples were viewed in bright field mode in a JEOL 200CX transmission electron microscope using an acceleration voltage of 200 kV. The cobalt particles were visible as darker units on the silica grains.

2.3.3.2 Atomic absorption spectroscopy

Atomic absorption is a spectroscopic technique for determining the catalyst composition. Each type of atom emits a characteristic spectrum that consists of a series of densely spaced spectral lines. This provides the basis for spectrographic analyses of the composition of the vaporised mixture of atoms.

Due to the hydroscopic nature of the cobalt nitrate precursor, it is necessary to verify the exact Co metal loading. 0.2g-0.3g of the reduced cobalt catalyst was wetted with a few drops of deionised water. A 40% HF solution was used to digest the sample. The sample was then diluted with deionised water to obtain a value that lay in the optimum range of the spectrometer (1-200 $\mu g / ml$). A Varian Spectra AA-30 spectrometer was used with an air/acetylene flame. Only a few interferences have been observed for cobalt in an air/acetylene flame. Ni, Cr, W in concentrations of 1000 $\mu g / ml$, Si will interfere at 200 $\mu g / ml$ and Cu and Mo at 500 $\mu g / ml$ (Welz, 1976). Calibration was done with cobalt nitrate in solution with and without HF added. Standards were made up to 50 mg/l, 80 mg/l, 100 mg/l and 159 mg/l.

2.3.4 Fischer-Tropsch Synthesis

2.3.4.1 Experimental set-up

The catalyst was tested under Fischer-Tropics conditions in a fixed bed reactor at a reaction temperature of 220 ^{0}C, total pressure of 15 bar and H_2:CO molar ratio of 2:1. The flowrates of CO and H_2 were controlled by a Brooks and a Unit mass flow controller to be 5 ml (STP)/min. and 10 ml (STP)/min respectively. The mass flow controllers were calibrated using bubble flow meters. The mixer in the reactant feed line consisted of a $^1/_4$-inch tube filled with small glass beads to ensure proper mixing of the feed. The function

of the 4-way valve was to switch from inert argon gas flowing over the catalyst bed to syngas at the start of the reaction. The pressure regulator and a needle valve automatically controlled argon's flowrate. When the syngas was flowing over the catalyst bed, argon was bypassed and served as a make-up gas to maintain a total pressure of 15 bar in the reactor. See figure 2.2

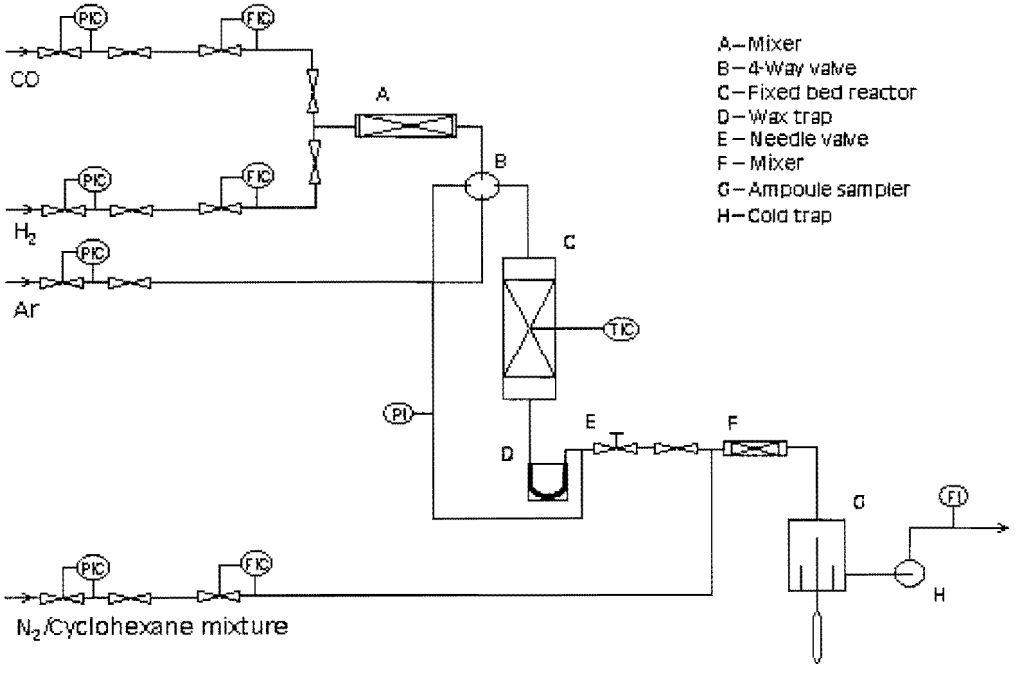

Figure 2.2: The flowsheet of the fixed bed reactor

The catalyst bed was packed in the region directly above the glass fritt and it was assumed to be in an isothermal region (see figure 2.3). Silonised glass wool was placed above the catalyst bed to keep the bed in place and glass beads on top of that to ensure proper mixing of the feed. The synthesis gas entered at the top of the reactor and the argon by-pass line entered at the side of the glass reactor and was mixed with the syngas and products at the reactor exit. The temperature inside the catalyst bed was measured with a thermocouple. The glass reactor was kept in place with a fitting and sealed by an o-ring. (see figure 2.3)

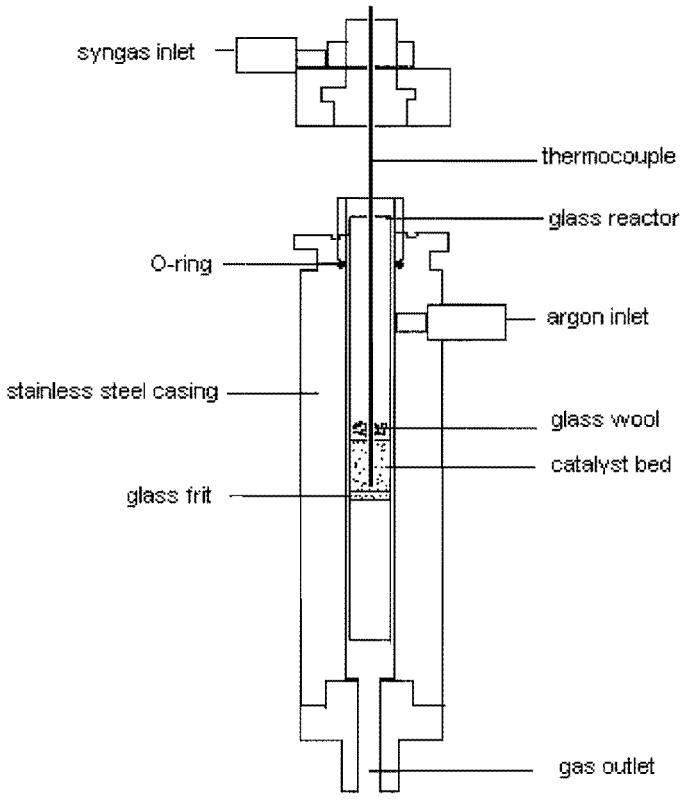

Figure 2.3: The glass reactor

The rig was tested for leaks by pressurizing it with hydrogen at 20 bar for 16 hours. For the reduction of the catalyst, the bed was first heated up to 200 °C with a 60 ml (STP)/min. argon to evaporate all the excess water. The catalyst was then heated to 360 ^{0}C at a heating rate of 2 ^{0}C/min and a flow of 60 ml (STP)/min of hydrogen and kept at 360 ^{0}C for 16 hours. The catalyst was then cooled down to 220 °C in argon, while the syngas on bypass and internal standard flowrates were stabilized.

A stainless U-tube filled with glass beads set at 180 ^{0}C ensured that the heavy waxes would be trapped and would not settle in the exit line and eventually cause a blockage. The reactor exit line was set at 190 ^{0}C to maintain the product mixture in the gas phase. The exit gas was passed through a cold trap set at room temperature to entrap hydrocarbons in the liquid phase at room temperature. The total flowrate was measured with a bubble flow meter.

2.3.4.2 Analyses of tailgas

Product analysis was carried out in two gas chromatographs. Conversion measurements were obtained through gas analysis on a Varian 3300 Series GC using a thermal conductivity detector (TCD) and an 80/100 Carbosieve II column. The organic product spectrum was analyzed in a Varian 3400 gas chromatograph (GC) with a flame ionisation detector (FID) and cryogenics installed. The cryogenic system installed on the FID GC made use of CO_2 enabling GC oven temperatures of –70 ^{0}C. The product separation was achieved using a 38-meter OV-1 type column with 0.25 μm film thickness and 0.25 mm ID. (see Appendix V)

Prior to reaction, the composition of the syngas stream was analysed by injecting samples with a Hamilton 0.5-ml syringe into the injector port of the TCD GC. When the bypass flows were stable, the four-way valve was switched to the reaction position. A Hamilton 5-ml syringe was used for direct injection into the FID GC while ampoule samples were taken for later analysis.

The reference gas used was 0.133% cyclohexane in nitrogen. Cyclohexane served as an internal standard in the analysis of the FT product spectrum, and was fed to the product line after the needle valve (see figure 2.2). FTS product samples were taken with the ampoule sampling technique at regular intervals.

3. RESULTS

3.1 Introduction

The effect of copper addition to the catalyst formulation of 20g Co/100g SiO_2 Fischer-Tropsch catalyst was investigated. The stepwise impregnation of different amounts of copper was done on a master batch of the impregnated cobalt catalyst to eliminate the reproducibility factor. The copper promoted catalysts were compared to the unpromoted catalyst, both with regard to their physical and chemical properties and their characteristics in Fischer-Tropsch synthesis. The co-impregnated (1g Cu/20g Co/100g SiO_2) and the copper catalyst (20g Cu/100g SiO_2) were also investigated under Fischer-Tropsch synthesis reaction conditions. The results obtained from the co-impregnated catalyst and the stepwise impregnated catalyst were, within experimental error, the same.

3.2 Physical and chemical properties

3.2.1 Atomic Absorption

The catalysts were synthesised by the incipient wetness impregnation method using an aqueous cobalt nitrate solution so as to produce a catalyst containing 16.67%(wt) of Co metal. Due to the hydroscopic nature of cobalt nitrate, the exact loading of Co metal had to be determined (see Table 3.1).

Table 3.1. Atomic Absorption Results

Catalyst	Wt % Cu	Wt % Co
0g Cu/20g Co/100g SiO_2	0.00 (0.00)*	13.1 (16.7)*
0.1g Cu/20g Co/100g SiO_2	0.08 (0.08)	14.2 (16.6)
0.5g Cu/20g Co/100g SiO_2	0.49 (0.41)	14.7 (16.6)
1g Cu/20g Co/100g SiO_2	0.74 (0.83)	14.2 (16.5)
2g Cu/20g Co/100g SiO_2	1.45 (1.60)	14.2 (16.4)

*Expected amounts in brackets

From the atomic absorption results it is clear that the amount of Co loaded was less than intended. This probably was due to the hydroscopic nature of cobalt nitrate as well as

copper nitrate. During impregnation less metal nitrate is added to the support which results in a lower weight percentage of Co and Cu than expected. As can be seen the expected weight percentage was about 16.5% for Co and the actual percentage of Co was in the 14% region. The Co metal loading of the different catalysts were found to be within the error of measurement. Catalysts from one master batch were used to impregnate different amounts of copper to eliminate the effect of different catalyst preparation procedures. The weight percentage of Cu loaded increased by a factor of 2 for each catalyst, as intended. The effect of small amounts of copper on the physical and chemical characterisation of the Co catalyst as well as FTS could be investigated.

3.2.2 BET surface area measurements and pore radius distributions

The characterisation of a catalyst ideally includes the measurement of the total surface area exposed by the support together with the measurement of the average pore diameter. The average pore diameter and the surface area of the support are related, and can be obtained from physical adsorption measurements. The total surface area of the support and the average pore diameter was measured using the BET method (see Table 3.2).

Table 3.2. Average pore size from BET

Catalyst	Area (m^2/g)	Pore size (nm)
SiO_2	286	8

3.2.3 CO chemisorption

Measurements were performed using a Micrometrics ASAP 2000C apparatus. The catalyst precursor was heated at 10 ^{0}C/min up to 360 ^{0}C under hydrogen, and kept at this temperature for 16 hours. After reduction the catalyst was degassed for 2 hours at 10^{-5} torr in order to eliminate chemisorbed hydrogen. The temperature was then lowered to 30 ^{0}C while maintaining the vacuum. The amount of CO adsorbed was determined using the dual isotherm technique. Chemisorption isotherms were measured between 50 - 400 mm Hg. After completing the first isotherm the weakly adsorbed CO was eliminated by evacuating the sample for 30 minutes at 10^{-5} torr and then the second isotherm was

obtained. The difference between the two isotherms gave the amount of CO irreversibly chemisorbed on the sample. The results are shown in Table 3.3.

Table 3.3: CO chemisorption of reduced catalyst

Catalyst	V_{CO}/g_{cat} (cm^3/g_{cat})	A_s (m^2/g_{cat})	Dispersion (%)	d_{avg} *(Co)* *(nm)*
0g Cu/20g Co/100g SiO_2	1.29	4.745	5.17	18.61
0.5g Cu/20g Co/100g SiO_2	1.35	4.969	5.07	18.99
1g Cu/20g Co/100g SiO_2	1.39	5.117	5.15	18.71
*1g Cu/20g Co/100g SiO_2	1.28	4.715	4.84	19.89
2g Cu/20g Co/100g SiO_2	1.32	4.859	4.96	19.42

*Co-impregnated

Taking into consideration the degree of reduction (100%) and the true metal loading obtained from AAS, the total number of exposed atoms can be calculated as well as the surface area (see Appendix II).

An alternative method to evaluate the volume of chemisorbed gas required to form a monolayer V_m, is to extrapolate the linear portion of the isotherm to zero pressure.

3.2.4 TEM results

TEM was used to look at the Co metal distribution on the support surface. Co metal could be seen as darker images on the SiO_2 support. TEM measures the actual size of a number of Co particles that can be seen on a very microscopic portion of the catalyst. The TEM images show that cobalt particles are present as clusters and the small metal crystals are separated from each other, indicating that the metal crystals are spread inside the pores of the support. From the TEM it could be seen that the metal were highly distributed over the support. (see Appendix IV) The average cluster size for all the catalysts were in the same region (see Table 3.4).

Table 3.4. Average Co cluster size from TEM measurements.

Catalyst	dp (nm)
0g Cu/20g Co/100g SiO_2	150
0.1g Cu/20g Co/100g SiO_2	100
0.5g Cu/20g Co/100g SiO_2	200
1g Cu/20g Co/100g SiO_2	175
2g Cu/20g Co/100g SiO_2	200

3.2.5 TPR results

The influence of different copper loadings on the reduction of the Co/SiO_2 catalyst was studied by temperature programmed reduction. Co undergoes a two step reduction; Co_3O_4 first reduces to CoO and then to cobalt metal. These two distinct peaks can be seen in the TPR spectra of the catalyst (calcined at 380 ^{o}C in N_2) with a normal heating rate of 10 ^{o}C/min. The hydrogen consumption associated with the reduction should be approximately 1.3 mol $H_{2,consumed}$/mol Co catalyst. Increasing the copper content from 0g Cu to 1g Cu per 20g Co/100g SiO_2 resulted in a clear shift in the temperature programmed reduction spectra. The hydrogen consumption peaks shifted to lower temperatures with an increase in copper content (see figure 3.1). Hydrogen consumption at higher temperatures (> 500 ^{0}C) can be attributed to strong-metal-support-interaction. There was no significant amount of hydrogen consumed above the second reduction peak indicating a low amount of strong metal support interaction.

Table 3.5: Hydrogen consumption during TPR and the first reduction peak temperatures for different Cu loadings.

Catalyst	*Total H_2:Co ratio (mole:mole)*	*T_{dec} (^{0}C)*
0g Cu/20g Co/100g SiO_2	1.29	290
0.5g Cu/20g Co/100g SiO_2	1.31	240
1g Cu/20g Co/100g SiO_2	1.30	205
2g Cu/20g Co/100g SiO_2	1.28	205

The amount of hydrogen consumed by the catalyst was apparently not influenced by the addition of copper even though this might have been expected (see Table 3.5).

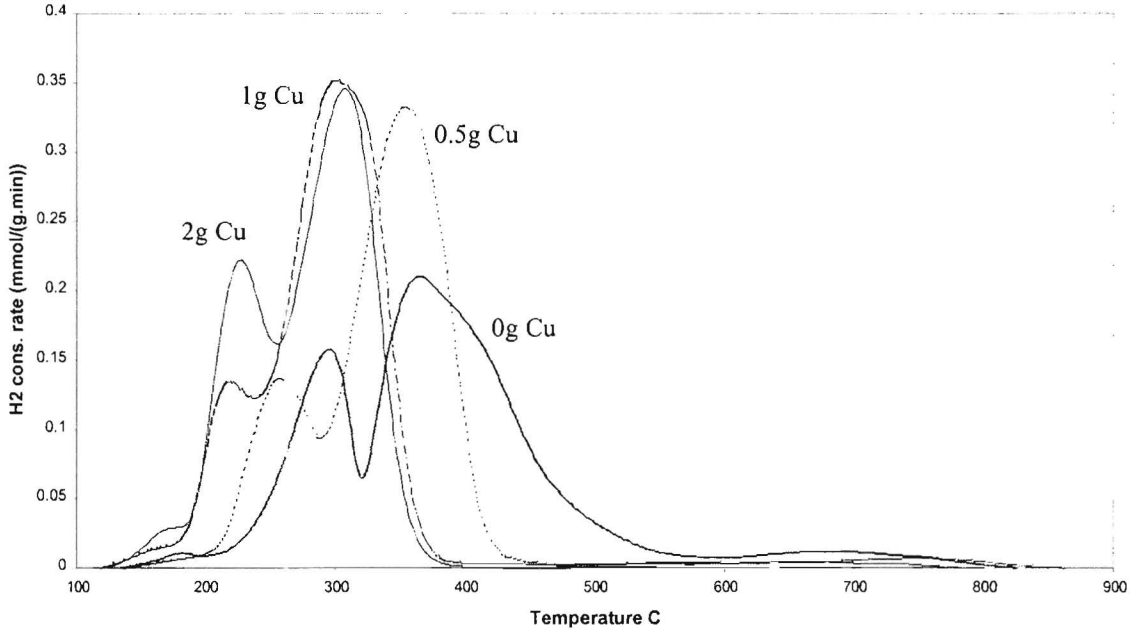

Figure 3.1 Effect of copper addition on the TPR spectra of Co/SiO_2 catalysts.

All catalysts were heated up to 1000 ^{0}C and kept at this temperature for 30 minutes to ensure total reduction of all the cobalt species. From the mass balance of the reduction process the H_2/Co ratio was found to be around 1.3 mol H_2/mol Co which corresponds to the stoichiometry of the process.

The TPR-spectra showed a clear shift in the peaks to lower temperatures with an increase in copper content. This was presumably due to a higher rate of reduction with an increase in copper content. H_2 adsorps dissociatively on copper metal and thereby acts a source of H_2 for the reduction of the cobalt oxide, and thereby increases the rate of reduction. The reduction of copper oxide can form a 'hot spot' and thereby increase the temperature of a certain region on the metal, and thereby also increase the rate of reduction.

3.3 Fischer-Tropsch synthesis

The catalysts were tested at 220 ^{0}C and 15 bar in a downflow fixed bed reactor. H_2 and CO were fed in a ratio of 2:1 at 30 ml (STP)/min. over 0.3g of catalyst. Gas samples were taken at 1hr., 4hrs., 16hrs., 20hrs. and 24 hrs. after the feed has been switched to the reactor. All the catalysts were reduced for 16 hrs. at 360 ^{0}C to ensure total reduction. A TPR was done on the reduced base case and it showed 100 % reduction. CO hydrogenation activity decreased with an increase in the amount of copper. A copper promoted catalyst was also prepared by means of co-impregnation and it showed the same result obtained for the stepwise impregnated catalyst. The activity of the 20g Cu/100g SiO_2 catalyst was less than 1% and mainly methanol was formed.

3.3.1 Time on stream behaviour

Figure 3.2 shows the time-on-stream behaviour The steady state yield of the volatile organic compounds decreased with increasing copper content. Steady state was assumed to be reached after 16 hours.

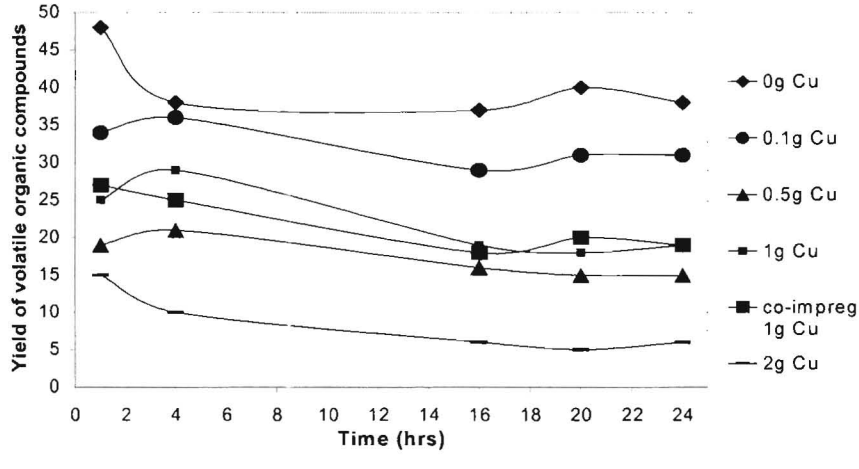

Figure 3.2: Yield of volatile organic compounds

(see Appendix III)

3.3.2 Activity and hydrocarbon yield

The total hydrocarbon yield was measured at steady state as a function of different copper loadings. A decrease in hydrocarbon yield with increase in copper loading was observed.

After 20 hours the hydrocarbon yield for 0g Cu/20g Co/100g SiO_2 was 38 C% and it decreased, with 2g Cu/20g Co/100g SiO_2 having the lowest hydrocarbon yield of 7% (see Table 3.6).

Table 3.6: Total hydrocarbon yield

Catalyst	Total yield (C%)
0g Cu/20g Co/100g SiO_2	38
0.1g Cu/20g Co/100g SiO_2	29
0.5g Cu/20g Co/100g SiO_2	13
1g Cu/20g Co/100g SiO_2	19
*1g Cu/20g Co/100g SiO_2	20
2g Cu/20g Co/100g SiO_2	7

*Co-impregnated

The addition of copper had a significant effect on the activity of the Co catalyst. The activity decrease with as much as 84% (mmol of CO/(gCo.min.)) with a 1.5 wt.% of copper (see table 3.7).

Table 3.7: Activity

Catalyst	Activity (mmol of CO/(g.min)	Activity (mmol of CO/(gCo.min)
0g Cu/20g Co/100g SiO_2	8.6E+02	6.6E+03
0.1g Cu/20g Co/100g SiO_2	6.4E+02	4.6E+03
0.5g Cu/20g Co/100g SiO_2	3.5E+02	2.4E+03
1g Cu/20g Co/100g SiO_2	4.4E+02	3.1E+03
*1g Cu/20g Co/100g SiO_2	4.3E+02	3.0E+03
2g Cu/20g Co/100g SiO_2	1.4E+02	1.0E+03

*Co-impregnated

3.3.3 Chain growth probability

The chain growth probability was measured at steady state as a function of different copper loadings. A decrease in chain growth probability with increase in copper loading was observed (see Table 3.8). After 20 hours the chain growth probability for 0g Cu/20g Co/100g SiO_2 was 0.84 and it decreased, with 2g Cu/20g Co/100g SiO_2 having the lowest chain growth probability of 0.72.

Table 3.8: Chain growth probability

Catalyst	Chain growth probability
0g Cu/20g Co/100g SiO_2	0.84
0.1g Cu/20g Co/100g SiO_2	0.81
0.5g Cu/20g Co/100g SiO_2	0.80
1g Cu/20g Co/100g SiO_2	0.78
2g Cu/20g Co/100g SiO_2	0.72

A plot of log $(n_i/\sum n_i)$ as a function of the carbon number was linear with deviations for methane, the C_2 fraction and carbon numbers greater than 15 (n_i is the molar fraction for each carbon fraction). see figure 3.3

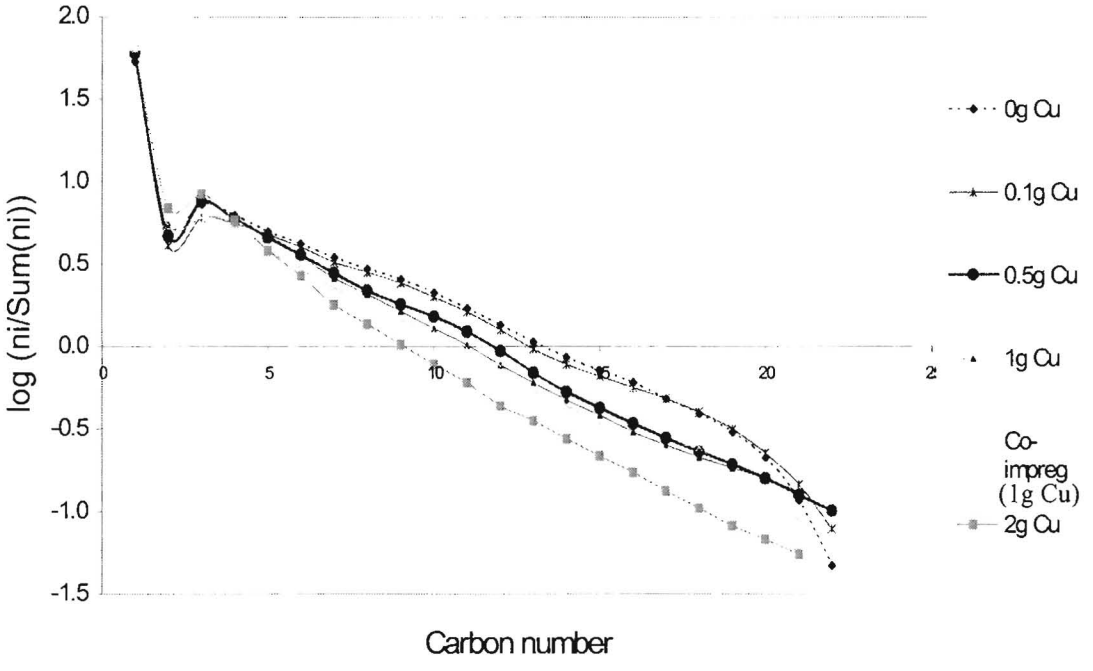

Figure 3.3: Anderson-Schultz-Flory-distribution

3.3.4 Selectivities

3.3.4.1 Methane selectivities

The addition of copper has a clear effect on the selectivities of the FT catalysts. With an increase in copper content the hydrogenating effect of the catalyst increased. This is indicated by the increase in the CH_4 selectivity and decrease in the olefinity of the C_3 fraction (see tables 3.9, 3.10 and 3.11)

Table 3.9: Methane selectivity

Catalyst	$S_{CH4}(C\%)$
0g Cu/20g Co/100g SiO_2	11
0.1g Cu/20g Co/100g SiO_2	12
0.5g Cu/20g Co/100g SiO_2	17
1g Cu/20g Co/100g SiO_2	19
2g Cu/20g Co/100g SiO_2	26

Table 3.10: Olefin to paraffin ratio of the C_2- and C_3-fraction

Catalyst	C_2-*fraction*	C_3-*fraction*
0g Cu/20g Co/100g SiO_2	0.42	2.8
0.1g Cu/20g Co/100g SiO_2	0.27	2.7
0.5g Cu/20g Co/100g SiO_2	0.36	2.3
1g Cu/20g Co/100g SiO_2	0.37	2.1
2g Cu/20g Co/100g SiO_2	0.34	1.8

Table 3.11: C_{5+} selectivities

Catalyst	$S_{C5+}(C\%)$
0g Cu/20g Co/100g SiO_2	74.4
0.1g Cu/20g Co/100g SiO_2	70.3
0.5g Cu/20g Co/100g SiO_2	63
1g Cu/20g Co/100g SiO_2	59
2g Cu/20g Co/100g SiO_2	44.5

3.3.4.2 Oxygenate selectivity

The oxygenate selectivity of the catalyst was investigated and this included mainly alcohols. Cu is known to be a methanol synthesis catalyst but operates at higher pressures and temperatures than FT conditions. The addition of copper had no clear effect on the methanol and ethanol selectivities (see Table 3.12)

Table 3.12: Alcohols

Catalyst	Methanol (mol %)	ethanol (mol %)
0g Cu/20g Co/100g SiO_2	3.75	1.41
0.1g Cu/20g Co/100g SiO_2	1.945	0.723
0.5g Cu/20g Co/100g SiO_2	1.968	0.698
1g Cu/20g Co/100g SiO_2	2.234	1.084
2g Cu/20g Co/100g SiO_2	3.86	1.46

4. DISCUSSION

The aim of the project was to test the influence of copper as a promoter on the cobalt catalyst. The TPR-spectra showed a clear shift in the peaks to lower temperatures with an increase in copper content, which indicates a higher rate of reduction. The catalyst characterisations showed no apparent effect on the physical and chemical properties of the Co catalyst. There was a significant influence on the Fischer-Tropsch performance of the catalyst. The activity of the cobalt catalyst decreased with an increase in copper loading.

4.1 Reproducibilty of results

Catalysts from one master batch were used to impregnate different amounts of copper to eliminate the effect of different catalyst preparation procedures. The amount of Cu loaded increased by a factor of 2 for each catalyst, as intended. Performing at least two mass balances under the same set of process conditions, checked the important issue of reproducibility of experimental data. Table 4.1 shows that product selectivities (hydrocarbon distribution and olefin selectivities) were similar for the mass balances. The error of the two runs are not bigger than 10% for the 5 different catalysts.

	Catalysts									
	0g Cu		**0.1g Cu**		**0.5g Cu**		**1g Cu**		**2g Cu**	
Y_{HC} (C%)	38.3	39.5	31.5	31.4	17.0	15.8	18.3	19.0	6.4	7.0
S_{CH4} (C%)	10.7	11.0	11.4	11.3	18.9	18.1	19.1	19.3	25.5	26.0
S_{C5+} (C%)	74.4	74.0	76.3	76.4	75.0	75.6	59	57.8	44.5	44.1
Olefin/parrafin C_3-fraction	2.8	2.81	2.82	2.82	2.29	2.32	2.2	2.2	1.9	2.0
Ethanol(mol%)	1.41	1.45	0.7	0.7	0.7	0.7	1.1	0.8	1.4	1.5

Table 4.1: Product selectivities at steady state for two runs of the same catalyst

4.2 Influence of copper promotion on the physical and chemical properties of the catalysts

4.2.1 TPR-spectra

The appearance of two distinct, different maxima in the TPR-spectra indicates the reduction of two different species. This indicates that the reduction of the calcined catalyst is a two-step process. The first peak could be ascribed to Co_3O_4 particles being reduced to CoO and the second peak the reduction of CoO to Co metal. All catalysts were heated up to 1000 ^{0}C and kept at this temperature for 30 minutes to ensure total reduction of all the cobalt species. From the mass balance of the reduction process the H_2/Co ratio was found to be around 1.3 mol H_2/mol Co which corresponds to the stoichiometry of the overall reduction.

The TPR-spectra showed a clear shift in the peaks to lower temperatures with an increase in copper content. This is due to a higher rate of reduction with an increase in copper content. It is proposed that H_2 adsorps dissociatively on copper and thereby acts as a source of H_2 for the reduction of the cobalt oxide, and thereby increases the rate of reduction. In addition, the reduction of the copper oxide may form a 'hot spot' and thereby increase the temperature of a certain region on the metal, and also increase the rate of reduction.

4.2.2 Metal cluster size and dispersion and effect of copper promotion on FT activity

Taking the amount of CO chemisorbed by the 0g copper catalyst as the base case, the effect of copper on the chemisorption of the catalyst could be studied qualitatively. The chemisorption of the different catalysts show no significant effect on the metal surface area as well as on the dispersion. This may be explained by the fact that copper also adsorbs CO and the increase in the amount of copper in the cobalt catalyst does not influence the overall chemisorption. Copper is a well known methanol catalyst and for this reason it also adsorbs CO. The TEM photographs also showed, within experimental error, no significant effect on the metal cluster size as well as dispersion.

During heating and/or catalytic reactions, the supported metal catalysts have a high tendency to sinter and thus to decrease the exposed surface area and surface free energy of the system. The extent of sintering depends on several parameters includng time of treatment, temperature, gas phase composition and the properties of the support and of the active phase. The formation of highly dispersed particles on a support is governed by nucleation and growth mechanisms. For sintering to occur particles or atoms, molecules or clusters of the active phase must become mobile. The Tamman temperature (K):

$$T_{Tam} \approx \frac{1}{2} T_{melt}^{bulk}$$

is considered to be sufficient to make atoms or ions of the bulk of a solid sufficiently mobile for bulk-to surface migrations [Ertl et. al.,1997]. The Hüttig temperature (K):

$$T_{Hut} \approx \frac{1}{3} T_{melt}^{bulk}$$

Is enough to make species already located on the surface sufficiently mobile to undergo agglomeration or sintering. With the melting temperature of Co: T_{melt} = 1768.15 K, the Tamman temperature is T_{Tam} = 884 K (611 ^{0}C) and the Hüttig temperature is T_{Hut} = 589 K (316 ^{0}C). With the melting temperature of Cu: T_{melt} = 1356 K (1083^{0}C), the Tamman temperature is T_{Tam} = 678 K (405 ^{0}C) and the Hüttig temperature is T_{Hut} = 452 K (179 ^{0}C). Therefore Cu has a higher tendency than Co to migrate to the surface, because of Cu metal's higher mobility. It is speculated that because the Cu is more mobile than Co the Cu 'decorates', i.e. spreads itself over the Co surface. This would result in a lowered amount of exposed Co surface atoms. Cobalt adsorbs CO dissociatively and is therefore active for FT synthesis, in contrast copper adsorbs CO associatively and is active for methanol formation [van der Laan, 1999]. This could explain why Cu addition lowered the observed FT activity without lowering the measured CO chemisorption.

The products showed a typical Anderson-Schultz-Flory-distribution with the alpha values decreasing with an increase in copper content (see table 3.9 and figure 3.3).
The deviations from ideal Anderson-Schultz-Flory-distribution are expected and are usually explained as follows:

- The higher methane mole fraction can be as a result of parallel formation reactions.

- Lower C_2 fraction, due to the high reactivity of ethene
- Higher mole fractions of the heavy fractions due to an increased readsorption of the highly reactive alpha-olefins

The alpha values were determined between carbon number 4 and carbon number 15 for all the catalysts. The reason for the decrease in the alpha values with increasing Cu content is not clear. It may be speculated that compared to cobalt the relative adsorption strengths of CO and H_2 on Cu are different. If H_2 adsorps relatively more strongly on Cu and if hydrogen spillover then occurs onto the Co surface, the latter would become more hydrogenating, resulting in lower olefin to parafin ratios (see Table 3.11) and an increase in the probability of chain termination, yielding the observed lower alpha values. The latter would result in an increase in CH_4 selectivity and a decrease in the C_{5+} selectivity (see figure 4.1).

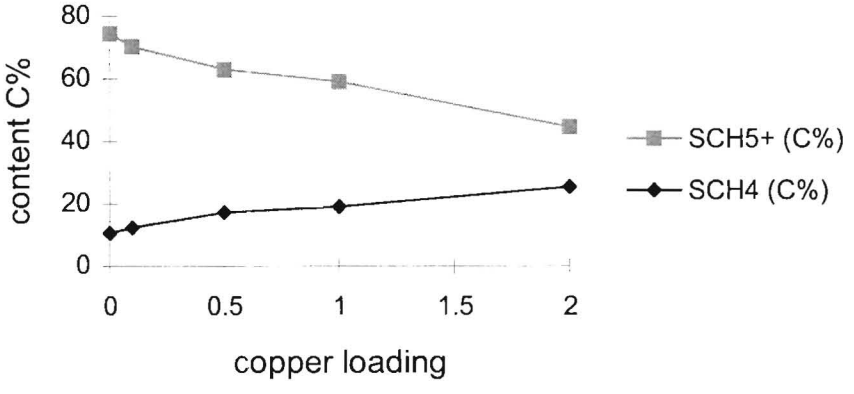

Figure 4.1: Methane and the C_{5+} selectivity

Olefin selectivity

The effect of copper promotion on olefin selectivity, expressed as a mole percent of linear olefins in the total hydrocarbon product of the same carbon number, is shown in figure 4.2

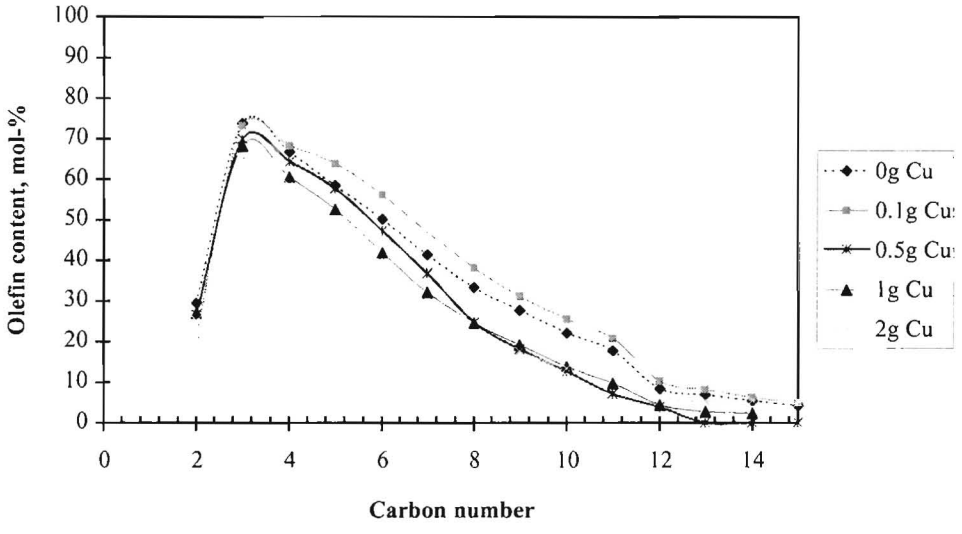

Figure 4.2: Effect of copper content on the olefin selectivity of the cobalt catalyst

For all the curves the olefin content increases from C_2 to C_3, and then decreases with increasing carbon number. This shape results from secondary hydrogenation of olefins. Ethylene is more reactive than other low molecular weight olefins, whereas the increase in the hydrogenaton activity (i.e. lower olefin content) of higher molecular weight olefins may be atributed to their increased reactivity or to a greater adsorptivity of long chain molecules. Copper promotion enhances the secondary hydrogenation of olefins, and the olefin content decreases with the copper loading as shown in figure 4.2. The increased hydrogenation activity has also been observed for the addition of copper to iron [Bukur, 1990].

Oxygenate selectivity

Oxygenates comprise only a small fraction of the products formed and consist primarly of n-alcohols and small amounts of aldehydes. No clearly discernible trends are observed in oxygenate selectivity as a function of copper concentration
(see table 3.13).

Activity of the Co catalyst

The addition of copper had a significant depressing effect on the activity of the catalyst (see section3.3.2). The pronounced suppression of activity when copper was added to a cobalt catalyst was observed by Storch in 1931 and Schwank in 1991. The reasons for the decrease in catalyst activity with the addition of copper are not clearly understood. A 20g Cu/100g SiO_2 (i.e. a Co free catalyst) was prepared and tested under FTS conditions. The activity of the copper catalyst was less than 0.5 %. If the copper hypothetically covers the surface of the cobalt catalyst (see section 4.2.2) there will be a very low FT catalyst activity. For this reason it is proposed that, because of the higher mobility of copper it will tend to cover the cobalt metal catalyst surface and thereby inhibit the catalyst activity. With an increase in the concentration of copper the more mobile copper is able to cover more of the active sites thus inhibiting the FTS activity (see Table 3.14).

5. REFERENCES

Adesina, A. A., *Appl. Catal. A: General* 138 (1996) 345-367.

Anderson, J. R., "Structure of Metallic Catalysts.", Academic Press, New York, 1975.

Anderson, R. B., Seligman, B., Schulz, J. F., Kelly, R., and Elliot, M. A., *Ind. Eng., Chem.,* 44 (1952) 391.

Anderson, R. B., "Catalysis IV.", Reinhold, New York, 1956.

Anderson, R. B., "The Fischer-Tropsch Synthesis", Academic Press, New York, 1984.

Arnoldy, P., Moulijn, J.A., *J. Catal.*, 93 (1995) 38.

Bartholomew, C. H., Pannell, R. B., and Butler, J. L., *J. Catal.*, 65 (1980) 335.

Bessel, S., *Appl. Catal., A:General*, 96 (1993) 253-268.

Boskovic, G. and Smith. K. J., *Catal. Today*, 37 (1997) 25.

Brady, R.C., and Petit, R., *J. Am. Chem. Soc.*, 103, (1981), 1287.

Bukur, B., and Mukesh, D., *Ind. Eng. Chem.Res.*, 29, (1990), 194

Claeys, M., Schulz., H., and Harms, S., *Stud. Surf. Sci. Catal.*, 107 (1997) 193.

Delmon, B., Grange, P., Preparation of catalysts IV, Elsevier, Amsterdam, 1987.

Dry, M. E., "Catalysis Science and Technology" Vol. 1, New York, 1981.

Dry, M. E., *Appl. Ind. Catal.*, 2 (1983) 167.

Dry, M. E., *Catal. Today*, 6(3) (1990) 186.

Dry, M. E., "Conversion of Syngas to Fuels and Chemicals.", I. C. on Catal. & Catalytic Processing, Cape Town. 1993.

Dry, M.E., *Appl. Cat A., General*, 138 (1996), 319

Ertl, G., Knozinger, H., Weitkamp, J., *Handbook of Heterogeneous Catalysis,* 1,2 (1997) 1,427

Feller, A., Claeys, M., van Steen, E., *J. Catal.*, 185 (1999) 120.

Fischer, H., and Tropsch, H., *Brennst. Chem.*, 4 (1923) 276.

Fischer, F., Tropsch, H., *Brennst. Chem.*, 7 (1926) 97.

Fischer, F., Tropsch, H., *Brennst. Chem.*, 16 (1935) 6.

Foger, K., *Catalysis Science and Technology.*, Vol 6., New York, 1985.

Friedman, S., Schlesinger, M.D., *US Mines Bull.*,(1964) 614

German Patent 293 787 (1913) BASF

Guerrero-Ruiz, A., Seulvelda-Escribano, A., Rodriguez-Ramos, I., *Appl. Catal. A: General* 120 (1994) 71

Harold, H. S., *The Chemistry of hydrocarbon fuels.*, Billing & Sons, Britain, 1990.

Iglesia, E., Reyes., S.C., and Madon, R. J., *J. Catal.*, 129 (1991) 238.

Iglesia, E., Reyes, S. C., Madon R. J., and Soled, S. L., *Advances in Catal.*, 39 (1993) 221.

Iglesia, E., Soled, S. L., Baumgartner, J. E., Reyes, S. C., *J. Catal.* 153 (1995) 108.

Iglesia, E., *Appl. Catal. A: General* 161 (1997) 59-78.

Kolbel, H., Ralek, M., *Catal. Rev. – Sci. Eng..*, 21 (1980) 225

Kolbel, H., Engelhardt, F., *Angew. Chem.* 64 (1953) 2

Kolbel, H., Ackerman, P., Ruschenbug, E., Langheim, R., Engelhardt, F., Beitrag zur Fischer-Tropsch Synthese on Eiensenkontakten. *Chem. Ing. Tech.* 23 (1951) 153

Kuipers E. W., Vinkenburg, I. H., and Oosterbeek, H., *J. Catal.*, 152 (1995) 137-146.

Martin, F., *Chem Fabriek,* 12 (1939) 233

Mirodatos, C., Brum Pereira, E., Gomez Cobo, A., Dalmon, J.A., Martin, G.A., *Topics Catal.* 2 (1995) 193

Orlov, E.I., *Zhur Russ.. Khim. Ob-va*, 40 (1908) 1588

Perego, C., Villa, P., *Catalysis Today* , 34 (1997) 281 "Catalyst preparation methods"

Pichler, H., "Advances in Catalysis.", Vol. 4, Academic Press, New York, 1952.

Pichler, H., "Advances in Catalysis.", Vol. 4, Academic Press, New York, 1952.

Pichler, H., Schulz, H., and Elstner, M., *Brennst. Chem.*, 48 (1967) 78.

Pichler, H., and Schulz, H., *Chem. Ing., Techn.* 42 (1970) 1162.

Quyoum, R., Berdini, V., Turner, M. L., Long, H. C., and Maitlis, P. M., *J. Catal.*, 173 (1998) 355.

Rao, V.U.S., Stiegel, G.J., Cinquegrane, G.J., Srivastave, R.D., *Fuel Process Technol.*, 30 (1992) 83

Reuel, R. C., and Bartholomew, C. H., *J. Catal.* 85 (1984) 78-88.

Rosynek, M. P., and Polansky, C. A., *Appl. Catal.*, 73 (1991) 97.

Sabatier, P., and Senderens, J. B., *Compte Rendus Hebd.*, 134 (1902) 514.

Schulz, H., and Claeys, M., *Appl. Catal. A: General,* 186 (1999) 71-90.

Scwank, J., *Stud. Surf. Sci. Catal.*, 64 (1991) 225

Sewel,G.S., Ph.D. Thesis, University of Cape Town, (1996)

Sie, S. T., Senden, M. M. G., and Van Wechem, H. M. H., *Catal. Today.*, 8 (1991) 371.

Sinfelt, J.H., Taylor, W.F., and Yates, D.J.C., *J. Phys. Chem.* 69, 95, 1965

Stern, D., Bell, A. T., and Heinneman, H., *Chem Eng. Sci.* 40 (1985) 1655.

Storch, H., Golumbic, N., and Anderson, R., "The Fischer-Tropsch and Related Syntheses." John Wiley & Sons, New York, 1951.

Tau, L. M., Dabbagh, H. A., and Davis, B. H., *Energy Fuels*, 4, 1990, 94.

Van der Laan, G.P.,Beenacres A.A.C.M., *Cat. Rev.-Sci. Eng.*, 41 (1999) 255

Vannice, M. A., *J. Catal.* , 37 (1975) 449.

Vannice, M. A., *J Catal.*, 50 (1977) 228.

Van Steen, E., PhD dissertation, *Elementarshritte der Fischer-Tropsch CO Hydrierung mit Eisen- und Kobaltkatalysatoren.* (1993).

Van Steen, E., Sewell., G. S, Makhote, A., Micklethwaite, C., Manstein, H., de Lange, M., and O'Connor, C. T., *J. Catal.*, 162 (1996) 220.

Wachs, I.E., Duyer, D.J., Iglesia, E., Characterisation of Fe, Fe-Cu and Fe-Ag Fischer-Tropsch catalysts., *Appl. Catal.* 12 (1984) 201

Wang, H.T., Chen, Y.W., and Goodwin, J.G., Zeolites, 4, (1984) 63-77.

Welz, B., Chemie, V., Atomic Absorption Spectroscopy, Weinheim, New York, 1976.

Zowtiak, J. M., and Bartholomew, C. H., *J. Catal.*, 83 (1983) 107.

Appendix I

TPR calibration and Sample calculation

The hydrogen concentration of the H_2 and N_2 gas mixture was caculated using a known mass of CuO, according o the following reaction stoichiometry:

$$CuO + H_2 \rightarrow Cu + H_2O$$

The CuO was placed in a quartz reactor described previously, and secured in the furnace. The thermal conductivity of 60 ml/min. N_2 and 60 ml/min. H_2 in N_2 were measured consecutively relative to a reference nitrogen gas stream flowing at 60 ml/min. The difference in the TCD measurement between the N_2 and the H_2 in N_2 gas mixure. During the TPR run, thr thermal conductivity of the exit stream is recorded. As hydrogen was consumed during copper reduction, the thermal conductivity of the exit gas changed reflecting the hydrogen consumption

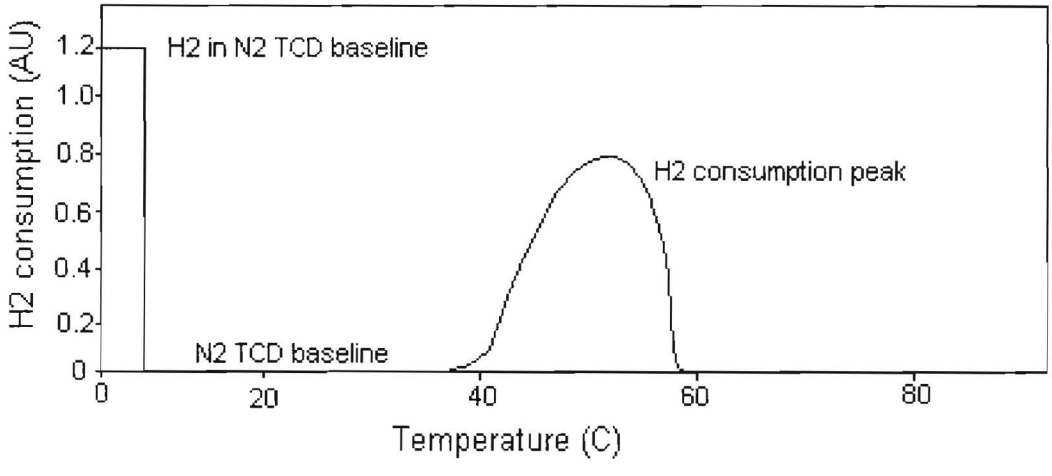

Figure AI.1: TPR of copper oxide

The hydrogen consumed in terms of the logged thermal conductivity acquired data was calculated using the trapezoidal rule given by the following expression:

$$H_2 \text{ consumption} = \sum_n (s_{n+1} + s_n) \times (t_{n+1} + t_n) \times 0.5$$

where s is the value logged for a given TCD reading and t is the time elapsed in minutes. The above expression was converted into mmols of hydrogen consumed on the assumption that the hydrogen concentration was 5%. On the basis, 1.020g, giving 1.340 mmols of Cu. As the stoichiometry of complete CuO reduction requires a 1:1 ratio of hydrogen to copper, the first guess of 5% for the hydrogen concentration was inaccurate.

H_2 concentration = 6.36 vol% H_2 in N_2.

All TPR runs used a similar procedure to obtain the hydrogen consumption, however for all other runs a hydrogen concentration of 6.36% was used.

Sample calculation

Figure AI-2 shows the TPR spectra obtained for the calcined catalyst precursors.

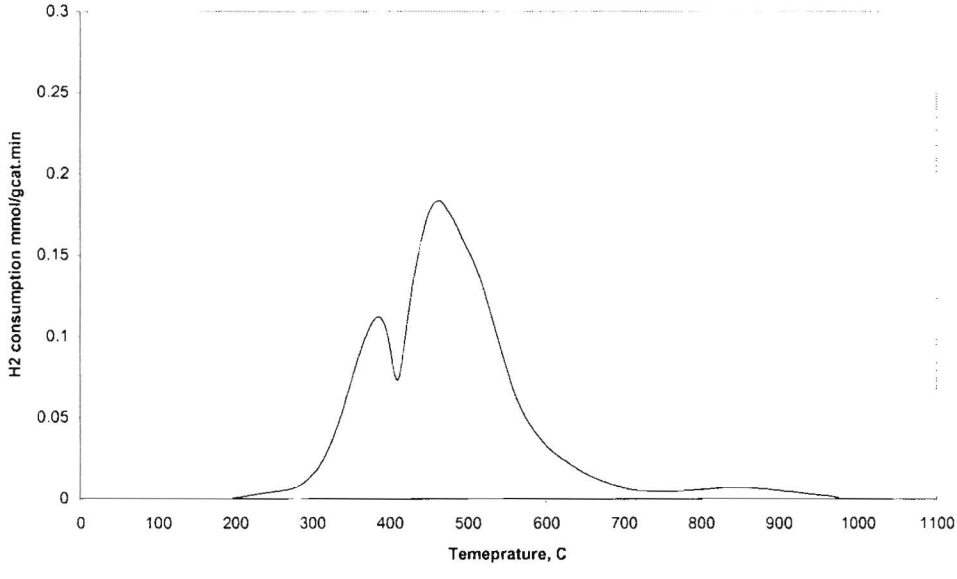

Figure AI-2. TPR spectra of calcined catalyst precursors (calcination: 380 ^{0}C for 6 hrs, TPR: 373 K-1273 K at 10 K/min in 60ml(NTP)/min 6.36% H_2/N_2).

Table AI-2. shows a typical portion of the spread sheet used to calculate the H_2/CO ratios

Mass of catalyst	0.13	0% H2	0.000001
Cobalt loading, mol-%	16.667	Max H2	0.0218
mmol Co	0.367656	H2-concentration	6.36
H2/Co, mol/mol	1.414489	Flowrate	60 ml/min
		Temperature	100
		n	25 ml/mmol
		molar Flow rate	2.4 mmol/min
		molar Flow H2	0.15264
		Total H2-uptake	3.407011
		H2-cons	0.520046 mmol

Table AI-2. Typical spread sheet used to calculate the H_2/CO ratios

Calculation of H_2/CO ratios from the TPR

For a 0.13 g of catalyst (mass after TPR), the number of mmols of cobalt was calculated using the atomic absorption results. Assuming the cobalt loading to be 16.67% then: number of

$$\text{mmols of cobalt} = \frac{0.13 \times 16.67}{58.933 \times 1000} = 0.36$$

The concentration of hydrogen in mmols was calculated in several steps:

Firstly a molar flow rate of hydrogen was obtained as follows:

$$22.414 \times \frac{273.15 + 100}{273.15} \times \frac{60 \times 6.36}{100} = 0.125 \text{ mmol/min}$$

The H_2 concentration was calculated by multiplying the molar flow rate by the total hydrogen consumption from the TCD signal:

$0.125 \times 3.67 = 0.46$ mmol H_2

Finally the H_2/CO ratio was calculated as follows : $\frac{0.46}{0.36} = 1.1$

Appendix II

Sample calculation of average particle size as obtained from CO chemisorption:

From chemisorption the difference between the two isotherms gave the amount of CO irreversibly chemisorbed , $V_{CO/gcat}$ = 1.289 $cm^3/g_{red.cat}$. Taking into consideration the degree of reduction (100%) and the true metal loading obtained from AAS (13.1 wt-%), the total number of exposed atoms can be calculated as well as the surface area.

Assume bridged chemisorbed species,

$$N_{Co} = \frac{1.289\ cm^3 CO/g_{cat} \times 2 \times 6.023 * 10^{23}}{22414} = 6.927 \times 10^{19}\ \text{atoms Co/g}_{cat}$$

1.289 = volume adsorbed (cm^3/g_{cat})

$6.022*10^{23}$ atoms in a molecule

22.414 m^3/kmol standard volume

The site density of fcc cobalt is 14.6 atoms.nm^2 [Sewell, 1996]. The metallic surface area can be determined as follows:

Surface area = $(6.927 \times 10^{19}$ Co atoms/$g_{cat})/(14.6$ atoms/$nm^2) \times 10^{-18} m^2/nm^2$

= 4.745 $m^2/\ g_{cat}$

The metallic dispersion is the number of metal atoms exposed, relative to the total number of metal atoms present in the sample. The number of reduced metal atoms can be determined by multiplying the total number of metal atoms in the catalyst sample by the extent of reduction.

$$\text{Dispersion} = \frac{6.927 * 10^{19}\ \text{atoms Co/g}_{cat}(exposed)}{1.339 * 10^{21}\ \text{Co/g}_{cat}(reduced)} * 100$$

= 5.17 %

The volume of reduced cobalt present on the reduced Co/SiO_2 catalyst is determined by using the following relationship, with density of 8.9 g/cm^3 [Sewel, 1996].

$$\text{Volume} = \frac{1.339 * 10^{21}\ \text{atoms}}{6.023 * 10^{23}\ \text{atoms/mol}} \times \frac{58.93 g/mol}{8.9 g/cm^3} \times 10^{-6} m^3/cm^3$$

$$= 1.47 * 10^{-8}\ \text{m}^3$$

The average particle dameter follows then from the volume surface relationship as:

$$\text{Average diameter} = 6 * \frac{1.47 * 10^{-8} m^3}{4.745 m^2} \times 10^9 nm/m$$

$$= 18.61\ \text{nm}$$

Appendix III

Sample calculation of conversion, yield and selectivity of the Fischer-Tropsch Synthesis reaction

The syngas feed of CO and H_2 were flowed over the catalyst in 1:2 ratio. Downstream of the reactor a stream of 0.336 % of toluene in nitrogen was flowed as an inert internal standard for both the conversion and organic yield calculations. It must be emphasised that cyclohexane is not a product of the Fischer-Tropsch synthesis. The conversion of carbon monoxide and hydrogen was calculated using a TCD gas chromatograph. Injecting known percentages of H2, CO and N2 gas mixture and noting the TCD response for each gas did the calibration. The relative response factor for CO and H_2 were obtained by dividing the response factor of the gas by the response factor of the nitrogen mixture.

Using the relative response factors, the areas obtained upon integration of the TCD signal following injection of gas from the product stream could be converted to molar ratios. As the molar fraction of the bypass was measured in the same way prior to the start of reaction, comparison of the bypass and reaction streams allowed calculation of the carbon monoxide and hydrogen conversions.

$$X_{CO} = \frac{\{(\frac{F_{CO}}{F_{N_2}})_{bypass} - (\frac{F_{CO}}{F_{N_2}})_{reaction}\}}{(\frac{F_{CO}}{F_{N_2}})_{bypass}}$$

with,

X = conversion

F = area obtained from GC analysis

The yield of total organic product and the selectivity of the product were determined using a FID gas chromatograph. The first step for the determination of the catalyst selectivity and the activity was the calculation of the molar flow rate of each volatile organic compound (VOC). Only the volatile organic compounds are present in the glass ampoules. The peak area of this

compound indicates the adjusted molar flow rate of cyclohexane. The molar flow rate of cyclohexane is:

$n_{cyclohexane} = x_{cyclohexane} \cdot \dot{V}_{ref}(NTP)/22.414$

with,

n = molar flow rate

x = molar fraction

V = volumetric flow rate

By comparing the peak areas of the other compounds with the reference gas peak, their molar flow rate could be determined. The peak areas of each compound are proportional to the amount of carbon atoms of the species analysed via FID. Therefore the molar flow rate of the compound j containing n carbon atoms is:

$n_j = n_{cyclohexane} (F_j/F_{cyclohexane}).(6/n)$

Adding up the molar flow rate of all compounds of one carbon number n yields n_n. The molar flow rate of VOC in the product stream is then:

$n_{VOC} = \Sigma n_n$

And the amount of carbon atoms in the VOC's is:

$N_{c,VOC} = nc_{cyclohexane} \{\Sigma (F_j)/F_{cyclohexane}\}.6$

For the ASF- diagram, the molar fraction of the group of compounds of one carbon number n (X_n) is determined:

$X_n = n_n/n_{VOC}.100\%$

The non-VOC's are products of the Fischer-Tropsch synthesis which are not present in the ampoules. The strong decrease of $\log(X_n)$ for n higher than 14 is caused by condensation in the wax trap. In order to compensate for this loss, the straight part of the ASF-plot (n = 7-12) is extrapolated to n = 100. The molar ratio of the group of products of the carbon number i, determined in that way is referred to as $X_{n,\,ASF}$. The molar flow rate of the group of molecules with the carbon number n (n>14) is then:

$$n_{n,ASF} = n_{VOC}\, x_{n,\,ASF}/100\%$$

The total molar flow rate of the Fischer-Tropsch synthesis product is:

$$n_{ASF} = n_{cyclohexane}\ \Sigma\{(F_j/F_{cyclohexane}).\ (6/n)\} + \Sigma\, n_{n,ASF}$$

The amount of carbon atoms in the real Fischer-Tropsch synthesis product is:

$$n_{c,ASF} = n_{cyclohexane}\ (\Sigma(F_j)/F_{cyclohexane}).\ 6+\Sigma\ (n_{n,ASF}..n)$$

That results in a yield Y_{ASF} of :

$$Y_{ASF} = n_{c,ASF}/\ (V_{CO}(NTP)/22.41)$$

Once the total yield of products from the ASF is determined, selectivities for a carbon number n can be calculated as follows:

$Cn/Y_{ASF}.100\%$

Appendix IV

TEM-photographs

The scaled TEM-photographs used for this study, are given in figures A4.1-A4.8:

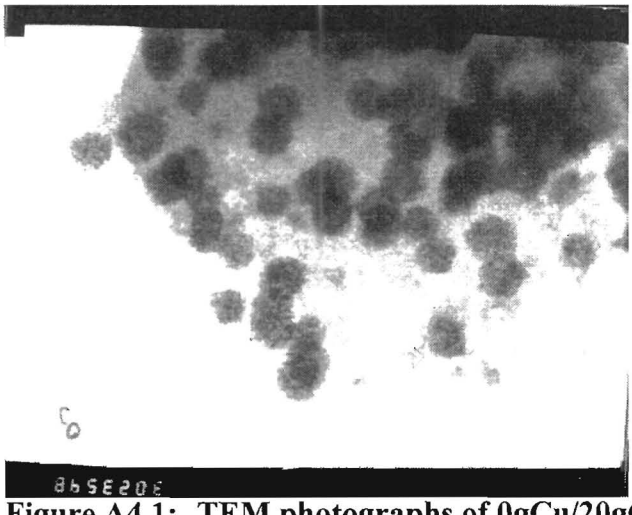

Figure A4.1: TEM photographs of 0gCu/20gCo/100gSiO$_2$ (stepwise impregnation, calcined at 380 ^{0}C for 6 hours in N_2 and reduced for 16 hours at 360 ^{0}C in H_2)
magnification: 30 000

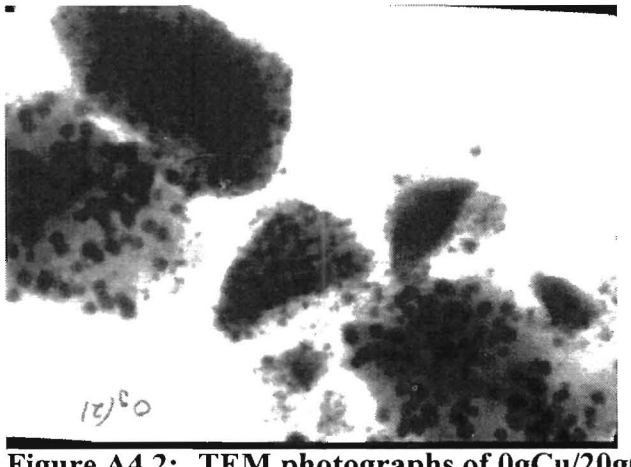

Figure A4.2: TEM photographs of 0gCu/20gCo/100gSiO$_2$ (stepwise impregnation, calcined at 380 ^{0}C for 6 hours in N_2 and reduced for 16 hours at 360 ^{0}C in H_2)
magnification: 10 000

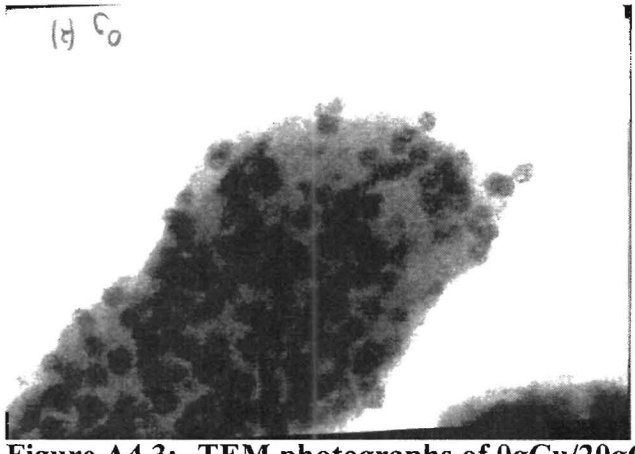

Figure A4.3: TEM photographs of 0gCu/20gCo/100gSiO_2 (stepwise impregnation, calcined at 380 ^{0}C for 6 hours in N_2 and reduced for 16 hours at 360 ^{0}C in H_2)
magnification: 30 000

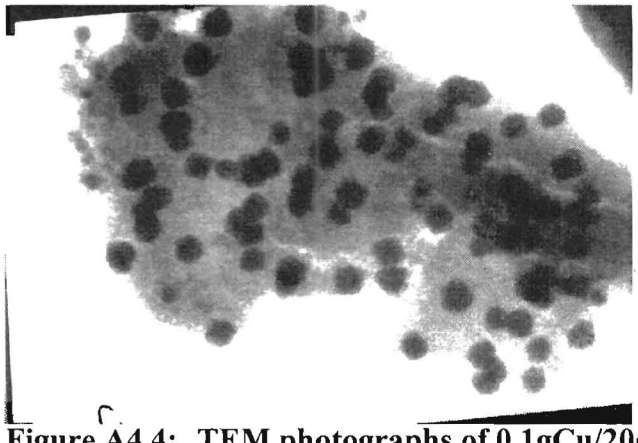

Figure A4.4: TEM photographs of 0.1gCu/20gCo/100gSiO_2 (stepwise impregnation, calcined at 380 ^{0}C for 6 hours in N_2 and reduced for 16 hours at 360 ^{0}C in H_2)
magnification: 20 000

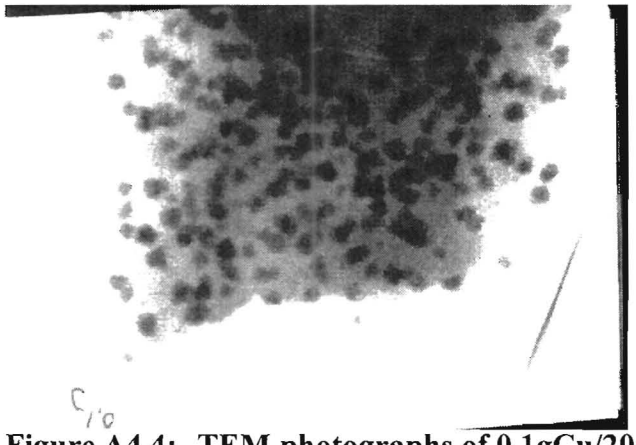

Figure A4.4: TEM photographs of 0.1gCu/20gCo/100gSiO_2 (stepwise impregnation, calcined at 380 ^{0}C for 6 hours in N_2 and reduced for 16 hours at 360 ^{0}C in H_2)
magnification: 20 000

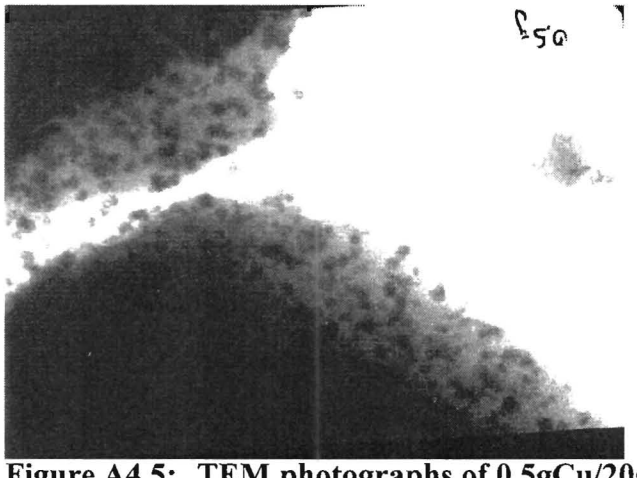

Figure A4.5: TEM photographs of 0.5gCu/20gCo/100gSiO_2 (stepwise impregnation, calcined at 380 ^{0}C for 6 hours in N_2 and reduced for 16 hours at 360 ^{0}C in H_2)
magnification: 10 000

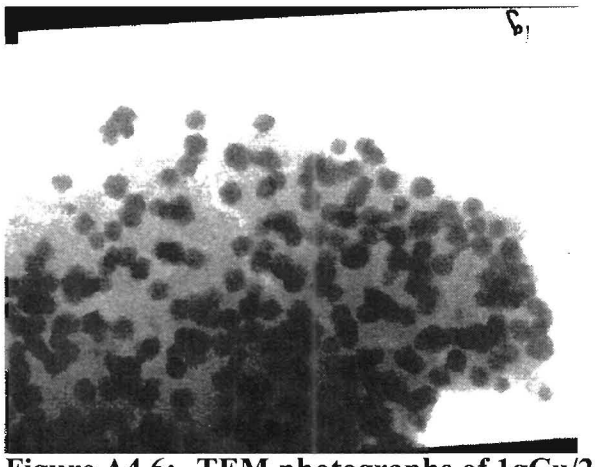

Figure A4.6: TEM photographs of 1gCu/20gCo/100gSiO_2 (stepwise impregnation, calcined at 380 ^{0}C for 6 hours in N_2 and reduced for 16 hours at 360 ^{0}C in H_2)
magnification: 20 000

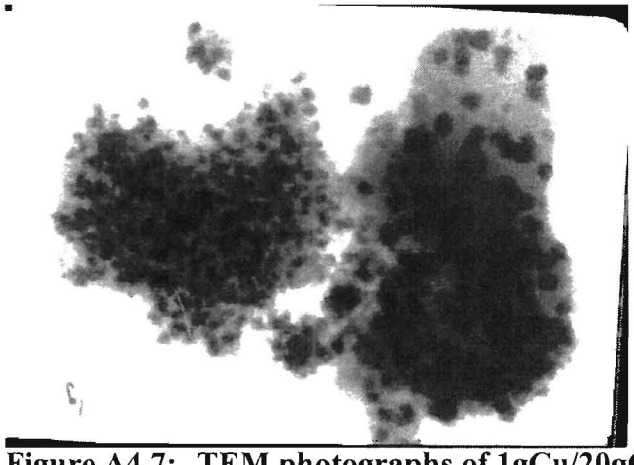

Figure A4.7: TEM photographs of 1gCu/20gCo/100gSiO_2 (stepwise impregnation, calcined at 380 ^{0}C for 6 hours in N_2 and reduced for 16 hours at 360 ^{0}C in H_2)
magnification: 20 000

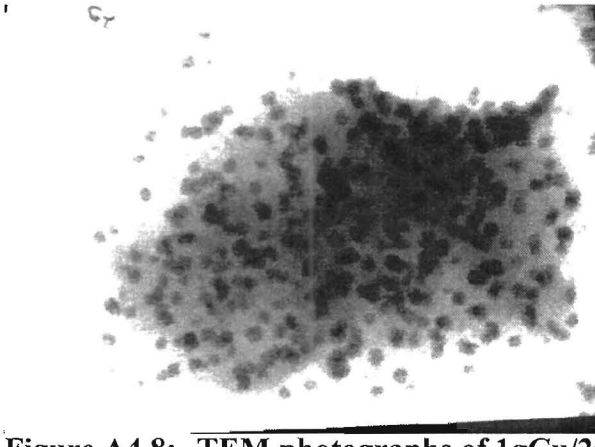

Figure A4.8: TEM photographs of 1gCu/20gCo/100gSiO_2 (stepwise impregnation, calcined at 380 ^{0}C for 6 hours in N_2 and reduced for 16 hours at 360 ^{0}C in H_2)
magnification: 20 000

Appendix V

Analysis of the FTS product samples
5.1 Parameters for the gaschromatography

Table 5.1: Gaschromatograph specifications

Gaschromatograph	Varian 3100
Column	CP-SilCB, 50*0.25, $d_f = 0.4$ μ m
Flush gas	Nitrogen
Carrier gas	Hydrogen

The behaviour of oxygen in the FID is taken account of by applying correction factors (Claeys, 1997) for the oxygenates in the product sample. These correction factors are:

Table 5.3: Correction factor for the peak area of oxygenates obtained by FID

Compound	Factor
Methanol	1.82
Ethanal	2.00
Ethanol	1.29
Propanal	1.50
n-propanol	1.18
n-butanol	1.13
n-butanal	1.33

Table 5.4: Temperature program for the gaschromatography of the FTS-product samples

Temperature (^{0}C)	Heating rate (^{0}C/min.)	Time of heating (min.)
-65	0	5
-65	15	2
-35	0	1
-35	10	3
-5	0	2.5
-5	2.5	12
25	5	51
280	0	60

5.2 Typical chromatogram

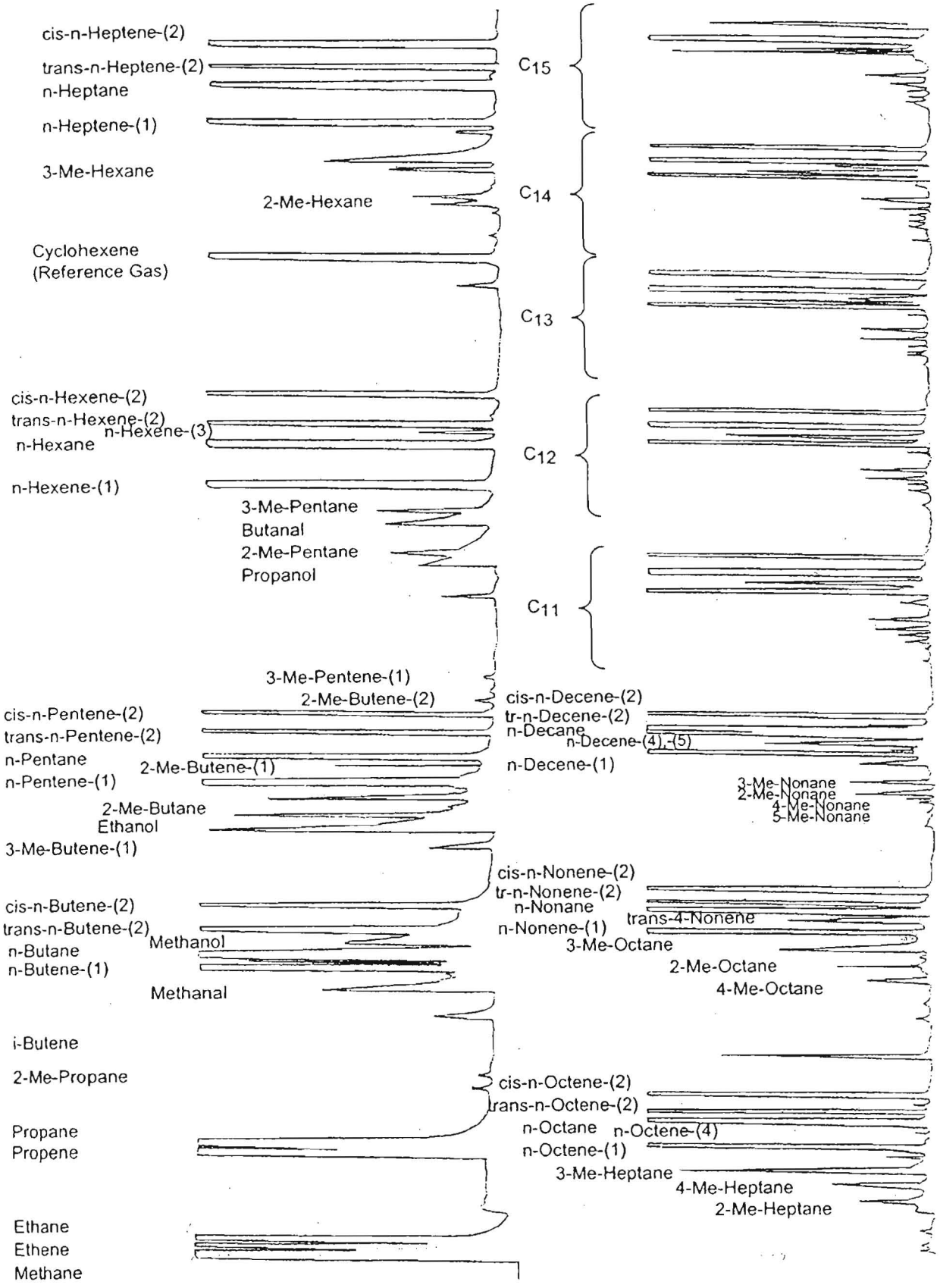

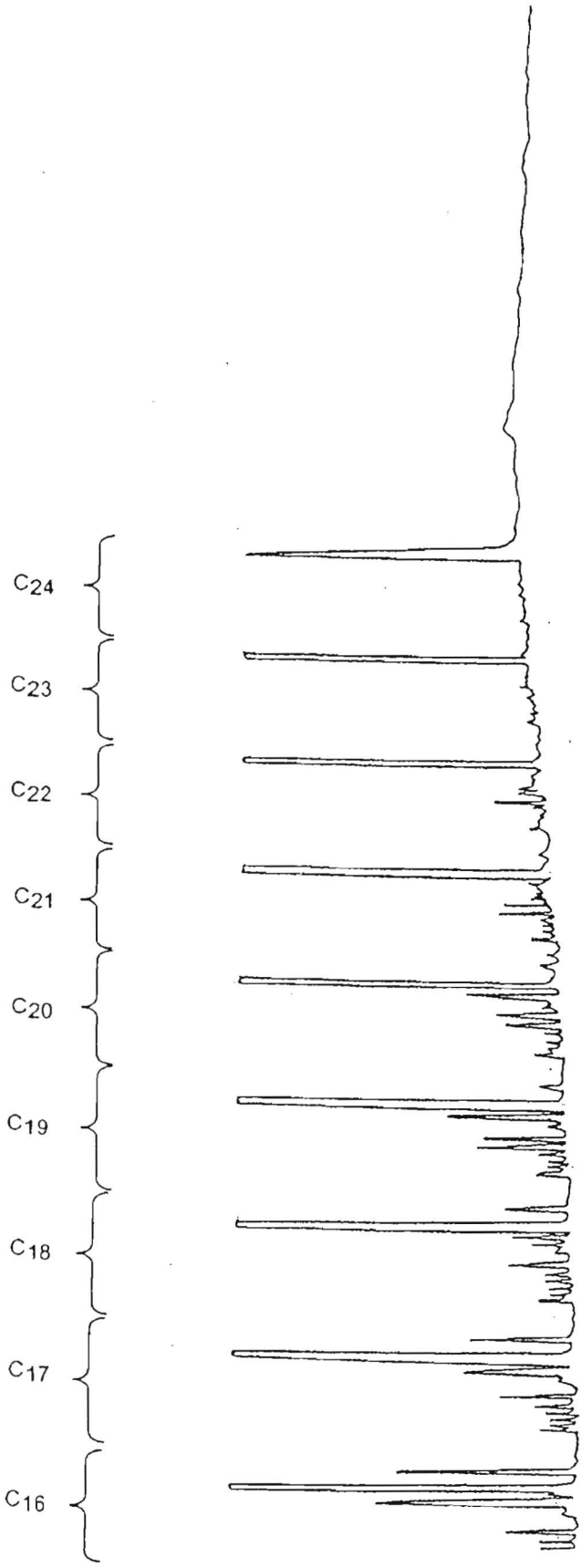
C24
C23
C22
C21
C20
C19
C18
C17
C16